A smoothing algorithm for joint input-state estimation in structural dynamics[☆,☆☆]

K. Maes[a,*], S. Gillijns[b], G. Lombaert[a]

[a] *KU Leuven, Department of Civil Engineering, Leuven, Belgium*
[b] *Siemens Industry Software NV, Leuven, Belgium*

Abstract

This paper presents a recursive algorithm where a time delay is considered in the estimation of the forces applied to a structure and the corresponding system states. In particular when the measured response is not collocated with the estimated forces, essential information on the estimated forces and/or system states is contained in the response at L consecutive time steps following the time step where the estimation is performed. The main focus in this paper is on the reduction in estimation incertainty that can be achieved by so-called smoothing, i.e. by considering a time delay in the estimation. When the calculation of the gain matrices is included in the recursive estimation, the calculation time of the algorithm largely increases with the time delay. It is shown that a prior calculation of the steady-state gain matrices allows for a significant reduction of the calculation time. The presented algorithm is first verified using numerical simulations. Next, a validation is performed using data obtained from a field test on a footbridge.

Keywords: joint input-state estimation, smoothing, time delay, force identification, response estimation, data fusion

1. Introduction

For many civil engineering structures, the dynamic loads cannot be directly measured. This is for example the case for wind loads acting on wind turbines or tall buildings, where data on such loads can be of interest for the design of future structures and the validation of load models prescribed by the Eurocodes or other design guidelines. In addition, it is practically and economically infeasible to measure the response of the structure at all locations of interest. For example, direct strain measurements in the tower of an offshore wind turbine below the water surface are difficult due to very harsh conditions. In these cases, inverse techniques can be applied for force and response estimation, hereby combining vibration data from a limited number of sensors with the information obtained from a dynamic model of the structure.

[☆] *Postprint submitted to Mechanical Systems and Signal Processing*
[☆☆] *Published version:* K. Maes, S. Gillijns, and G. Lombaert. A smoothing algorithm for joint input-state estimation in structural dynamics. *Mechanical Systems and Signal Processing*, 98:292–309, 2018.
https://doi.org/10.1016/j.ymssp.2017.04.047

[*] Corresponding author. Tel.: +32 (0) 16 32 25 73.
Email address: kristof.maes@kuleuven.be (K. Maes)

A wide variety of system inversion algorithms for force and state/response estimation has been proposed in the literature, tackling the system inversion problem in the frequency or time domain. Within the time domain approaches, a distinction can be made between deterministic approaches [1, 2, 3] and recursive filtering and smoothing approaches [4, 5, 6]. Filtering algorithms predict the input and states at time step k from the (known) response measured from time step 0 up to time step k, i.e. no delay is applied in the estimation. Note that only the response at time step k is explicitly used in the estimation of the input and/or states at the same time step k. Through recursion, the estimates at time step k depend on the response at all previous time steps, however. If a delay L is adopted in the estimation, i.e. the response from time step 0 to $k + L$ is used to (recursively) estimate the input and states at time step k, with $L > 0$, the estimation algorithm is classified as a smoothing algorithm. Smoothing algorithms can alternatively be classified as a specific type of moving horizon estimation (MHE) algorithms, which use the observations within a predefined time window (k to $k + L$) to estimate unknown variables, e.g. the system states [7]. Whereas MHE algorithms generally use (iterative) optimization to minimize the estimation uncertainty for separate time windows, smoothing algorithms implicitly optimize the solution through the choice of the gain matrices, which depend on the assumed noise statistics. Both filtering and smoothing algorithms are generally less computationally expensive than MHE algorithms, making them particularly suited for continuous health monitoring of structures over their lifetime. Because MHE algorithms are based on iterative optimization, the formulation of the system inversion problem is more general and allows including a priori information on the solution, however.

Recently, much focus has gone to joint input-state estimation, where the forces applied to the structure and the corresponding system states are simultaneously estimated. Joint input-state estimation is mostly performed by use of recursive Kalman filter based techniques [8, 9, 10, 11, 12, 13]. The conditions for (instantaneous) system inversion have been extensively documented in the literature [14, 15, 16]. Floquet and Barbot [17] showed that these conditions can be relaxed by allowing some delay in the estimation. Recently, Hsieh [18] developed a time delayed joint input-state estimation algorithm as an extension of an existing recursive three-step filtering algorithm [19].

This paper presents a recursive smoothing algorithm where a time delay is considered in joint input-state estimation. The developed approach is similar to that given in [18] and [20], but with a different filtering structure. The smoothing algorithm can be applied for force identification and response estimation and is an extension of a state-of-the-art filtering algorithm for joint input-state estimation [10, 13]. Where recent work on time-delayed system inversion has mainly focused on the relaxation of the invertibility criteria through the introduction of a time delay [18, 20], this paper mainly focuses on the reduction in estimation uncertainty. It is shown by numerical simulations that introducing a time delay in the estimation allows to significantly reduce the estimation uncertainty due to measurement noise in the case where the data originates from sensors that are not collocated with the estimated forces. It is also investigated how the calculation time of the algorithm increases with the time delay assumed in the estimation. A steady-state initialization is proposed to enable a significant speed-up of the calculations. The presented algorithm is validated using data obtained from a field test on a footbridge. This allows to investigate the influence of modeling errors in the estimation, which are inevitable when dealing with real structures.

The outline of the paper is as follows. Section 2 presents the smoothing algorithm for joint input-state estimation and its application for response estimation. Next, Section 3 shows an illustration of the algorithm based on numerical simulations for a cantilever steel beam. Section 4 presents

a validation of the smoothing algorithm using data obtained from a field test on a footbridge. Finally, in Section 5, the work is concluded.

2. Mathematical formulation

2.1. System model

Consider the following linear discrete-time combined deterministic-stochastic state-space description of a system:

$$\mathbf{x}_{[k+1]} = \mathbf{A}\mathbf{x}_{[k]} + \mathbf{B}\mathbf{p}_{[k]} + \mathbf{w}_{[k]} \tag{1}$$

$$\mathbf{d}_{[k]} = \mathbf{G}\mathbf{x}_{[k]} + \mathbf{J}\mathbf{p}_{[k]} + \mathbf{v}_{[k]} \tag{2}$$

where $\mathbf{x}_{[k]} \in \mathbb{R}^{n_\mathrm{s}}$ is the state vector, $\mathbf{d}_{[k]} \in \mathbb{R}^{n_\mathrm{d}}$ is the measured output vector, and $\mathbf{p}_{[k]} \in \mathbb{R}^{n_\mathrm{p}}$ is the input vector, to be estimated, with n_s the number of system states, n_d the number of outputs, and n_p the number of inputs. The system matrices $\mathbf{A}$, $\mathbf{B}$, $\mathbf{G}$, and $\mathbf{J}$ are assumed to be known. System noise is represented by the process noise vector $\mathbf{w}_{[k]} \in \mathbb{R}^{n_\mathrm{s}}$ and measurement noise vector $\mathbf{v}_{[k]} \in \mathbb{R}^{n_\mathrm{d}}$.

2.2. Smoothing algorithm

The system under consideration is described by Eqs. (1) and (2). Consider a vector $\mathbf{d}_{L[k]} \in \mathbb{R}^{(L+1)n_\mathrm{d}}$ that contains the response $\mathbf{d}_{[k]}$ over $L+1$ consecutive time steps ($L \geq 0$):

$$\mathbf{d}_{L[k]} \triangleq \begin{bmatrix} \mathbf{d}_{[k]} \\ \mathbf{d}_{[k+1]} \\ \vdots \\ \mathbf{d}_{[k+L]} \end{bmatrix} \tag{3}$$

Similar definitions are used for the input vector $\mathbf{p}_{L[k]}$ and the noise vectors $\mathbf{w}_{L[k]}$ and $\mathbf{v}_{L[k]}$. It is readily obtained from Eqs. (1), (2), and (3) that:

$$\mathbf{d}_{L[k]} = \boldsymbol{\mathcal{O}}_L \mathbf{x}_{[k]} + \boldsymbol{\mathcal{H}}_L \mathbf{p}_{L[k]} + \boldsymbol{\mathcal{N}}_L \mathbf{w}_{L-1[k]} + \mathbf{v}_{L[k]} \tag{4}$$

where $\boldsymbol{\mathcal{O}}_L \in \mathbb{R}^{(L+1)n_\mathrm{d} \times n_\mathrm{s}}$ and $\boldsymbol{\mathcal{H}}_L \in \mathbb{R}^{(L+1)n_\mathrm{d} \times (L+1)n_\mathrm{p}}$ denote the extended observability matrix and the Toeplitz matrix, respectively, defined by:

$$\boldsymbol{\mathcal{O}}_L \triangleq \begin{bmatrix} \mathbf{G} \\ \mathbf{GA} \\ \mathbf{GA}^2 \\ \vdots \\ \mathbf{GA}^L \end{bmatrix}, \quad \boldsymbol{\mathcal{H}}_L \triangleq \begin{bmatrix} \mathbf{J} & \mathbf{0} & \mathbf{0} & \dots & \mathbf{0} \\ \mathbf{GB} & \mathbf{J} & \mathbf{0} & \dots & \mathbf{0} \\ \mathbf{GAB} & \mathbf{GB} & \mathbf{J} & \dots & \mathbf{0} \\ \vdots & \vdots & \vdots & \ddots & \vdots \\ \mathbf{GA}^{L-1}\mathbf{B} & \mathbf{GA}^{L-2}\mathbf{B} & \mathbf{GA}^{L-3}\mathbf{B} & \dots & \mathbf{J} \end{bmatrix} \tag{5}$$

The matrix $\boldsymbol{\mathcal{N}}_L$ is defined recursively as follows:

$$\boldsymbol{\mathcal{N}}_0 \triangleq \mathbf{0}, \quad \boldsymbol{\mathcal{N}}_1 \triangleq \begin{bmatrix} \mathbf{0} \\ \mathbf{G} \end{bmatrix}, \quad \boldsymbol{\mathcal{N}}_k \triangleq \begin{bmatrix} \mathbf{0} & \mathbf{0} \\ \boldsymbol{\mathcal{O}}_{k-1} & \boldsymbol{\mathcal{N}}_{k-1} \end{bmatrix} \quad (k \geq 2) \tag{6}$$

where $\boldsymbol{\mathcal{N}}_0 \in \mathbb{R}^{n_\mathrm{d} \times n_\mathrm{s}}$ and $\boldsymbol{\mathcal{N}}_k \in \mathbb{R}^{(k+1)n_\mathrm{d} \times k n_\mathrm{s}}$ for $k > 0$.

Similarly to smoothing approaches that have been previously presented in [18] and [20], the recursive smoothing algorithm proposed in this paper estimates the system states $\mathbf{x}_{[k]}$ and the forces $\mathbf{p}_{[k]}$ from a set of response measurements $\mathbf{d}_{[k]}$ obtained at $L+1$ consecutive time steps, contained in the vector $\mathbf{d}_{L[k]}$. A state estimate $\hat{\mathbf{x}}_{[k|l]}$ is defined as an estimate of $\mathbf{x}_{[k]}$, given the output sequence $\mathbf{d}_{[n]}$, with $n = 0, 1, \ldots, l$. The corresponding error covariance matrix, denoted by $\mathbf{P}_{\mathrm{x}[k|l]}$, is defined as:

$$\mathbf{P}_{\mathrm{x}[k|l]} \triangleq \mathbb{E}\left[(\mathbf{x}_{[k]} - \hat{\mathbf{x}}_{[k|l]})(\mathbf{x}_{[k]}^\mathrm{T} - \hat{\mathbf{x}}_{[k|l]}^\mathrm{T})\right] \tag{7}$$

An input estimate $\hat{\mathbf{p}}_{[k|l]}$ and its error covariance matrix $\mathbf{P}_{\mathrm{p}[k|l]}$ are defined similarly.

In the derivation of the smoothing algorithm, the noise processes $\mathbf{w}_{[k]}$ and $\mathbf{v}_{[k]}$ are assumed to be zero mean and white, with known covariance matrices $\mathbf{Q}$, $\mathbf{R}$, and $\mathbf{S}$, defined by:

$$\mathbb{E}\left[\begin{pmatrix}\mathbf{w}_{[k]} \\ \mathbf{v}_{[k]}\end{pmatrix}\begin{pmatrix}\mathbf{w}_{[l]}^\mathrm{T} & \mathbf{v}_{[l]}^\mathrm{T}\end{pmatrix}\right] = \begin{bmatrix}\mathbf{Q} & \mathbf{S} \\ \mathbf{S}^\mathrm{T} & \mathbf{R}\end{bmatrix}\delta_{[k-l]} \tag{8}$$

with $\mathbf{R} > 0$, $\begin{bmatrix}\mathbf{Q} & \mathbf{S} \\ \mathbf{S}^\mathrm{T} & \mathbf{R}\end{bmatrix} \geq 0$, where $\mathbb{E}[\cdot]$ indicates the expectation operator.

A summary of the smoothing algorithm is presented in the following. The reader is referred to Appendix A for the derivation of the algorithm.

The smoothing algorithm is initialized using an initial state estimate vector $\hat{\mathbf{x}}_{[0|L-1]}$ and its error covariance matrix $\mathbf{P}_{\mathrm{x}[0|L-1]}$. The estimate $\hat{\mathbf{x}}_{[0|L-1]}$ is assumed unbiased and independent of the noise processes $\mathbf{w}_{[k]}$ and $\mathbf{v}_{[k]}$ for all k. The algorithm proceeds by computing the force and state estimates recursively in two steps, i.e. the input estimation step and state estimation step:

Input estimation

$$\mathbf{P}_{\mathrm{xw}[k]} = \sum_{i=1}^{\min(k,L)} \left(\left(\prod_{j=1}^{i-1}\left(\mathbf{A} - \mathbf{K}_{L[k-j]}\boldsymbol{\mathcal{O}}_L\right)\right)\left(\left(\breve{\mathbf{I}}_{n_\mathrm{s}} - \mathbf{K}_{L[k-i]}\boldsymbol{\mathcal{N}}_L\right)\mathbf{Q}_L^i - \mathbf{K}_{L[k-i]}\mathbf{S}_L^{-i^\mathrm{T}}\right)\right) \tag{9}$$

$$\mathbf{P}_{\mathrm{xv}[k]} = \sum_{i=1}^{\min(k,L)} \left(\left(\prod_{j=1}^{i-1}\left(\mathbf{A} - \mathbf{K}_{L[k-j]}\boldsymbol{\mathcal{O}}_L\right)\right)\left(\left(\breve{\mathbf{I}}_{n_\mathrm{s}} - \mathbf{K}_{L[k-i]}\boldsymbol{\mathcal{N}}_L\right)\mathbf{S}_L^i - \mathbf{K}_{L[k-i]}\mathbf{R}_{L+1}^i\right)\right) \tag{10}$$

$$\begin{aligned}\bar{\mathbf{R}}_{[k]} = {} & \boldsymbol{\mathcal{O}}_L\mathbf{P}_{\mathrm{x}[k|k+L-1]}\boldsymbol{\mathcal{O}}_L^\mathrm{T} + \mathbf{R}_{L+1}^0 + \boldsymbol{\mathcal{N}}_L\mathbf{Q}_L^0\boldsymbol{\mathcal{N}}_L^\mathrm{T} + \boldsymbol{\mathcal{N}}_L\mathbf{S}_L^0 + \mathbf{S}_L^{0^\mathrm{T}}\boldsymbol{\mathcal{N}}_L^\mathrm{T}\ldots \\ & + \boldsymbol{\mathcal{O}}_L\mathbf{P}_{\mathrm{xw}[k]}\boldsymbol{\mathcal{N}}_L^\mathrm{T} + \boldsymbol{\mathcal{N}}_L\mathbf{P}_{\mathrm{xw}[k]}^\mathrm{T}\boldsymbol{\mathcal{O}}_L^\mathrm{T} + \boldsymbol{\mathcal{O}}_L\mathbf{P}_{\mathrm{xv}[k]} + \mathbf{P}_{\mathrm{xv}[k]}^\mathrm{T}\boldsymbol{\mathcal{O}}_L^\mathrm{T}\end{aligned} \tag{11}$$

$$\mathbf{M}_{L[k]} = \breve{\mathbf{I}}_{n_\mathrm{p}}\left(\boldsymbol{\mathcal{H}}_L^\mathrm{T}\bar{\mathbf{R}}_{[k]}^{-1}\boldsymbol{\mathcal{H}}_L\right)^\dagger\boldsymbol{\mathcal{H}}_L^\mathrm{T}\bar{\mathbf{R}}_{[k]}^{-1} \tag{12}$$

$$\hat{\mathbf{p}}_{[k|k+L]} = \mathbf{M}_{L[k]}\left(\mathbf{d}_{L[k]} - \boldsymbol{\mathcal{O}}_L\hat{\mathbf{x}}_{[k|k+L-1]}\right) \tag{13}$$

$$\mathbf{P}_{\mathrm{p}[k|k+L]} = \mathbf{M}_{L[k]}\bar{\mathbf{R}}_{[k]}\mathbf{M}_{L[k]}^\mathrm{T} \tag{14}$$

State estimation

$$\bar{\mathbf{S}}_{[k]} = \mathbf{A}\mathbf{P}_{\mathrm{x}[k|k+L-1]}\boldsymbol{\mathcal{O}}_L^{\mathrm{T}} + \breve{\mathbf{I}}_{n_\mathrm{s}}\mathbf{Q}_L^0\boldsymbol{\mathcal{N}}_L^{\mathrm{T}} + \breve{\mathbf{I}}_{n_\mathrm{s}}\mathbf{S}_L^0 + \mathbf{A}\mathbf{P}_{\mathrm{xw}[k]}\boldsymbol{\mathcal{N}}_L^{\mathrm{T}} + \breve{\mathbf{I}}_{n_\mathrm{s}}\mathbf{P}_{\mathrm{xw}[k]}^{\mathrm{T}}\boldsymbol{\mathcal{O}}_L^{\mathrm{T}} + \mathbf{A}\mathbf{P}_{\mathrm{xv}[k]} \tag{15}$$

$$\bar{\mathbf{T}}_{[k]} = \mathbf{A}\mathbf{P}_{\mathrm{x}[k|k+L-1]}\mathbf{A}^{\mathrm{T}} + \mathbf{Q} + \mathbf{A}\mathbf{P}_{\mathrm{xw}[k]}\breve{\mathbf{I}}_{n_\mathrm{s}}^{\mathrm{T}} + \breve{\mathbf{I}}_{n_\mathrm{s}}\mathbf{P}_{\mathrm{xw}[k]}^{\mathrm{T}}\mathbf{A}^{\mathrm{T}} \tag{16}$$

$$\mathbf{K}_{L[k]} = \bar{\mathbf{S}}_{[k]}\bar{\mathbf{R}}_{[k]}^{-1} - \left(\bar{\mathbf{S}}_{[k]}\bar{\mathbf{R}}_{[k]}^{-1}\boldsymbol{\mathcal{H}}_L - \breve{\mathbf{B}}\right)\left(\boldsymbol{\mathcal{H}}_L^{\mathrm{T}}\bar{\mathbf{R}}_{[k]}^{-1}\boldsymbol{\mathcal{H}}_L\right)^{\dagger}\boldsymbol{\mathcal{H}}_L^{\mathrm{T}}\bar{\mathbf{R}}_{[k]}^{-1} \tag{17}$$

$$\hat{\mathbf{x}}_{[k+1|k+L]} = \mathbf{A}\hat{\mathbf{x}}_{[k|k+L-1]} + \mathbf{K}_{L[k]}(\mathbf{d}_{L[k]} - \boldsymbol{\mathcal{O}}_L\hat{\mathbf{x}}_{[k|k+L-1]}) \tag{18}$$

$$\mathbf{P}_{\mathrm{x}[k+1|k+L]} = \mathbf{K}_{L[k]}\bar{\mathbf{R}}_{[k]}\mathbf{K}_{L[k]}^{\mathrm{T}} - \mathbf{K}_{L[k]}\bar{\mathbf{S}}_{[k]}^{\mathrm{T}} - \bar{\mathbf{S}}_{[k]}\mathbf{K}_{L[k]}^{\mathrm{T}} + \bar{\mathbf{T}}_{[k]} \tag{19}$$

where † denotes the Moore Penrose pseudo inverse of a matrix, $\sum_{i=1}^{j}(\cdot) \triangleq \mathbf{0}$ for $i > j$, $\prod_{i=1}^{j}(\cdot) \triangleq \mathbf{I}$ for $i > j$, $\breve{\mathbf{I}}_{n_\mathrm{s}} = [\mathbf{I}_{n_\mathrm{s}} \;\; \mathbf{0} \;\; \ldots \;\; \mathbf{0}] \in \mathbb{R}^{n_\mathrm{s}\times Ln_\mathrm{s}}$, with $\mathbf{I}_{n_\mathrm{s}} \in \mathbb{R}^{n_\mathrm{s}\times n_\mathrm{s}}$ an identity matrix, $\breve{\mathbf{I}}_{n_\mathrm{p}} = [\mathbf{I}_{n_\mathrm{p}} \;\; \mathbf{0} \;\; \ldots \;\; \mathbf{0}] \in \mathbb{R}^{n_\mathrm{p}\times(L+1)n_\mathrm{p}}$, with $\mathbf{I}_{n_\mathrm{p}} \in \mathbb{R}^{n_\mathrm{p}\times n_\mathrm{p}}$ an identity matrix, and $\breve{\mathbf{B}} = [\mathbf{B} \;\; \mathbf{0} \;\; \ldots \;\; \mathbf{0}] \in \mathbb{R}^{n_\mathrm{s}\times(L+1)n_\mathrm{p}}$. The extended noise covariance matrices $\mathbf{Q}_L^i \in \mathbb{R}^{Ln_\mathrm{s}\times Ln_\mathrm{s}}$, $\mathbf{R}_{L+1}^i \in \mathbb{R}^{(L+1)n_\mathrm{d}\times(L+1)n_\mathrm{d}}$ and $\mathbf{S}_L^i \in \mathbb{R}^{Ln_\mathrm{s}\times(L+1)n_\mathrm{d}}$ are defined as:

$$\begin{aligned}
\mathbf{Q}_L^i &\triangleq \mathbb{E}\left[\mathbf{w}_{L-1[k-i]}\mathbf{w}_{L-1[k]}^{\mathrm{T}}\right] = \mathrm{diag}_L^i(\mathbf{Q},\mathbf{Q},\ldots,\mathbf{Q}) \\
\mathbf{R}_{L+1}^i &\triangleq \mathbb{E}\left[\mathbf{v}_{L[k-i]}\mathbf{v}_{L[k]}^{\mathrm{T}}\right] \qquad = \mathrm{diag}_{L+1}^i(\mathbf{R},\mathbf{R},\ldots,\mathbf{R}) \\
\mathbf{S}_L^i &\triangleq \mathbb{E}\left[\mathbf{w}_{L-1[k-i]}\mathbf{v}_{L[k]}^{\mathrm{T}}\right] \qquad = [\mathrm{diag}_L^i(\mathbf{S},\mathbf{S},\ldots,\mathbf{S}),\mathbf{0}] \qquad \text{for } i \geq 0 \\
&\qquad\qquad\qquad\qquad\quad = [\mathbf{0},\mathrm{diag}_L^{i+1}(\mathbf{S},\mathbf{S},\ldots,\mathbf{S})] \qquad \text{for } i < 0
\end{aligned} \tag{20}$$

where $\mathrm{diag}_j^i(\cdot)$ denotes a block matrix with the j matrices between the brackets on the i-th block diagonal below the main diagonal and zeros elsewhere.

The gain matrices $\mathbf{M}_{[k]}$ and $\mathbf{K}_{[k]}$ are determined such that – in absence of modeling errors – the input estimates $\hat{\mathbf{p}}_{[k|k+L]}$ and state estimates $\hat{\mathbf{x}}_{[k|k+L]}$ are minimum variance and unbiased [10] (see also Appendix A). The uncertainty on the force and state estimates, as given by the trace of the error covariance matrices, $\mathrm{tr}(\mathbf{P}_{\mathrm{p}[k|k+L]})$ and $\mathrm{tr}(\mathbf{P}_{\mathrm{x}[k+1|k+L]})$, is minimized, and the error on the estimated forces $\hat{\mathbf{p}}_{[k|k+L]}$ and states $\hat{\mathbf{x}}_{[k+1|k+L]}$ does not depend on the actual forces $\mathbf{p}_{L[k]}$. Finally, note that for $L = 0$ the force and state estimates in Eqs. (13) and (18) are identical to those obtained from the filtering algorithm presented in [13].

2.3. Response estimation

Consider a vector $\mathbf{d}_{\mathrm{e}[k]} \in \mathbb{R}^{n_{\mathrm{d,e}}}$ of output quantities that are to be identified from the estimated forces and states through response estimation, a.k.a. virtual sensing. This vector $\mathbf{d}_{\mathrm{e}[k]}$, hereafter referred to as the vector of extrapolated output quantities, is described by the following (discrete-time) output equation:

$$\mathbf{d}_{\mathrm{e}[k]} = \mathbf{G}_\mathrm{e}\mathbf{x}_{[k]} + \mathbf{J}_\mathrm{e}\mathbf{p}_{[k]} + \mathbf{v}_{\mathrm{e}[k]} \tag{21}$$

The matrices $\mathbf{G}_\mathrm{e} \in \mathbb{R}^{n_{\mathrm{d_e}}\times n_\mathrm{s}}$ and $\mathbf{J}_\mathrm{e} \in \mathbb{R}^{n_{\mathrm{d_e}}\times n_\mathrm{p}}$ relate to the extrapolated output quantities and are therefore different from the matrices $\mathbf{G}$ and $\mathbf{J}$ in Eq. (2) that relate to the measured output

quantities. The measurement noise vector $\mathbf{v}_{\mathrm{e}[k]}$ in Eq. (21) accounts for modeling errors and unknown excitation (see also [13]).

From the estimated state vector $\hat{\mathbf{x}}_{[k|k+L-1]}$ and force vector $\hat{\mathbf{p}}_{[k|k+L]}$, the extrapolated response $\mathbf{d}_{\mathrm{e}[k]}$ can be estimated using the following modified output equation:

$$\hat{\mathbf{d}}_{\mathrm{e}[k|k+L]} = \mathbf{G}_{\mathrm{e}}\hat{\mathbf{x}}_{[k|k+L-1]} + \mathbf{J}_{\mathrm{e}}\hat{\mathbf{p}}_{[k|k+L]} \tag{22}$$

Under the assumption of white noise processes $\mathbf{w}_{[k]}$, $\mathbf{v}_{[k]}$, and $\mathbf{v}_{\mathrm{e}[k]}$, the error covariance matrix $\mathbf{P}_{\mathrm{d_e}[k|k+L]}$ corresponding to the response estimate $\hat{\mathbf{d}}_{\mathrm{e}[k|k+L]}$ is given by:

$$\begin{aligned}
\mathbf{P}_{\mathrm{d_e}[k|k+L]} &\triangleq \mathbb{E}\left[(\mathbf{d}_{\mathrm{e}[k]} - \hat{\mathbf{d}}_{\mathrm{e}[k|k+L]})(\mathbf{d}_{\mathrm{e}[k]}^{\mathrm{T}} - \hat{\mathbf{d}}_{\mathrm{e}[k|k+L]}^{\mathrm{T}})\right] \\
&= \mathbf{G}_{\mathrm{e}}\mathbf{P}_{\mathrm{x}[k|k+L-1]}\mathbf{G}_{\mathrm{e}}^{\mathrm{T}} + \mathbf{J}_{\mathrm{e}}\mathbf{P}_{\mathrm{p}[k|k+L]}\mathbf{J}_{\mathrm{e}}^{\mathrm{T}} + \mathbf{R}_{\mathrm{e}} + \mathbf{G}_{\mathrm{e}}\mathbf{P}_{\mathrm{xp}[k|k+L]}\mathbf{J}_{\mathrm{e}}^{\mathrm{T}} \ldots \\
&\quad + \mathbf{J}_{\mathrm{e}}\mathbf{P}_{\mathrm{px}[k|k+L]}\mathbf{G}_{\mathrm{e}}^{\mathrm{T}} + \mathbf{G}_{\mathrm{e}}\mathbf{P}_{\mathrm{xv_e}[k]} + \mathbf{P}_{\mathrm{v_ex}[k]}\mathbf{G}_{\mathrm{e}}^{\mathrm{T}} + \mathbf{J}_{\mathrm{e}}\mathbf{P}_{\mathrm{pv_e}[k]} + \mathbf{P}_{\mathrm{v_ep}[k]}\mathbf{J}_{\mathrm{e}}^{\mathrm{T}}
\end{aligned} \tag{23}$$

where $\mathbf{R}_{\mathrm{e}} \in \mathbb{R}^{n_{\mathrm{d,e}} \times n_{\mathrm{d,e}}}$ represents the covariance matrix of the (white) noise process $\mathbf{v}_{\mathrm{e}[k]}$:

$$\mathbb{E}\left[\mathbf{v}_{\mathrm{e}[k]}\mathbf{v}_{\mathrm{e}[l]}^{\mathrm{T}}\right] = \mathbf{R}_{\mathrm{e}}\delta_{[k-l]} \tag{24}$$

The covariance matrices $\mathbf{P}_{\mathrm{xp}[k|k+L]}$ and $\mathbf{P}_{\mathrm{px}[k|k+L]}$ are given by:

$$\begin{aligned}
\mathbf{P}_{\mathrm{xp}[k|k+L]} =& \mathbf{P}_{\mathrm{px}[k|k+L]}^{\mathrm{T}} \triangleq \mathbb{E}\left[(\mathbf{x}_{[k]} - \hat{\mathbf{x}}_{[k|k+L-1]})(\mathbf{p}_{[k]}^{\mathrm{T}} - \hat{\mathbf{p}}_{[k|k+L]}^{\mathrm{T}})\right] \\
=& -\left(\mathbf{P}_{\mathrm{x}[k|k+L-1]}\boldsymbol{\mathcal{O}}_L^{\mathrm{T}} + \mathbf{P}_{\mathrm{xw}[k]}\boldsymbol{\mathcal{N}}_L^{\mathrm{T}} + \mathbf{P}_{\mathrm{xv}[k]}\right)\mathbf{M}_{L[k]}^{\mathrm{T}}
\end{aligned} \tag{25}$$

The covariance matrices $\mathbf{P}_{\mathrm{xv_e}[k]}$, $\mathbf{P}_{\mathrm{v_ex}[k]}$, $\mathbf{P}_{\mathrm{pv_e}[k]}$, and $\mathbf{P}_{\mathrm{v_ep}[k]}$ are given by:

$$\mathbf{P}_{\mathrm{xv_e}[k]} = \mathbf{P}_{\mathrm{v_ex}[k]}^{\mathrm{T}} \triangleq \mathbb{E}\left[\tilde{\mathbf{x}}_{[k|k+L-1]}\mathbf{v}_{\mathrm{e}[k]}^{\mathrm{T}}\right] \tag{26}$$

$$= \sum_{i=1}^{\min(k,L)} \left(\left(\prod_{j=1}^{i-1}\left(\mathbf{A} - \mathbf{K}_{L[k-j]}\boldsymbol{\mathcal{O}}_L\right)\right)\left(\left(\breve{\mathbf{I}}_{n_{\mathrm{s}}} - \mathbf{K}_{L[k-i]}\boldsymbol{\mathcal{N}}_L\right)\mathbf{S}_{\mathrm{c}}^{i^{\mathrm{T}}} - \mathbf{K}_{L[k-i]}\mathbf{R}_{\mathrm{c}}^{i^{\mathrm{T}}}\right)\right)$$

$$\mathbf{P}_{\mathrm{pv_e}[k]} = \mathbf{P}_{\mathrm{v_ep}[k]}^{\mathrm{T}} \triangleq \mathbb{E}\left[\tilde{\mathbf{p}}_{[k|k+L]}\mathbf{v}_{\mathrm{e}[k]}^{\mathrm{T}}\right] \tag{27}$$

$$= -\mathbf{M}_{L[k]}\left(\boldsymbol{\mathcal{O}}_L\mathbf{P}_{\mathrm{xv_e}[k]} + \boldsymbol{\mathcal{N}}_L\mathbf{S}_{\mathrm{c}}^{0^{\mathrm{T}}} + \mathbf{R}_{\mathrm{c}}^{0^{\mathrm{T}}}\right)$$

The extended noise covariance matrices $\mathbf{R}_{\mathrm{c}}^{i} \in \mathbb{R}^{n_{\mathrm{d,e}} \times (L+1)n_{\mathrm{d}}}$ and $\mathbf{S}_{\mathrm{c}}^{i} \in \mathbb{R}^{n_{\mathrm{d,e}} \times Ln_{\mathrm{s}}}$ are block matrices with the matrices $\mathbf{R}_{\mathrm{c}} \in \mathbb{R}^{n_{\mathrm{d,e}} \times n_{\mathrm{d}}}$, and $\mathbf{S}_{\mathrm{c}} \in \mathbb{R}^{n_{\mathrm{d,e}} \times n_{\mathrm{s}}}$ in block column $i+1$, respectively, where $\mathbf{R}_{\mathrm{c}}$ and $\mathbf{S}_{\mathrm{c}}$ represent the covariance matrices of the (white) noise processes:

$$\mathbb{E}\left[\mathbf{v}_{\mathrm{e}[k]}\mathbf{v}_{[l]}^{\mathrm{T}}\right] = \mathbf{R}_{\mathrm{c}}\delta_{[k-l]}, \text{ and } \mathbb{E}\left[\mathbf{v}_{\mathrm{e}[k]}\mathbf{w}_{[l]}^{\mathrm{T}}\right] = \mathbf{S}_{\mathrm{c}}\delta_{[k-l]} \tag{28}$$

3. Illustration

This section shows an illustration of the smoothing algorithm proposed in Section 2 using numerical simulations for a cantilever steel beam.

3.1. Cantilever beam

The structure under consideration is a cantilever steel beam, shown in Fig. 1. The same structure has been considered previously in [13]. The beam has a length of 1 m and rectangular cross section with a width of 50.8 mm and a height of 25.4 mm. The Young's modulus and material density are taken as 210 GPa and 7750 kg/m^3, respectively.

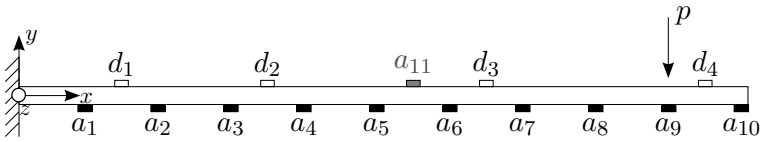

Fig. 1: Side view of the cantilever beam, including the force and sensor configuration (p: force, a_i: accelerometer i, and d_i: displacement sensor i).

The beam is modeled using a two-dimensional finite element (FE) model with 100 Euler-Bernoulli beam elements. Shear deformation is not accounted for. Only bending in the vertical plane is considered. The first four natural frequencies obtained from the beam model are 21.4 Hz, 133.7 Hz, 374.0 Hz, and 731.6 Hz. The corresponding bending mode shapes are shown in Fig. 2. A modal damping ratio of 2.5% is assumed for the four modes.

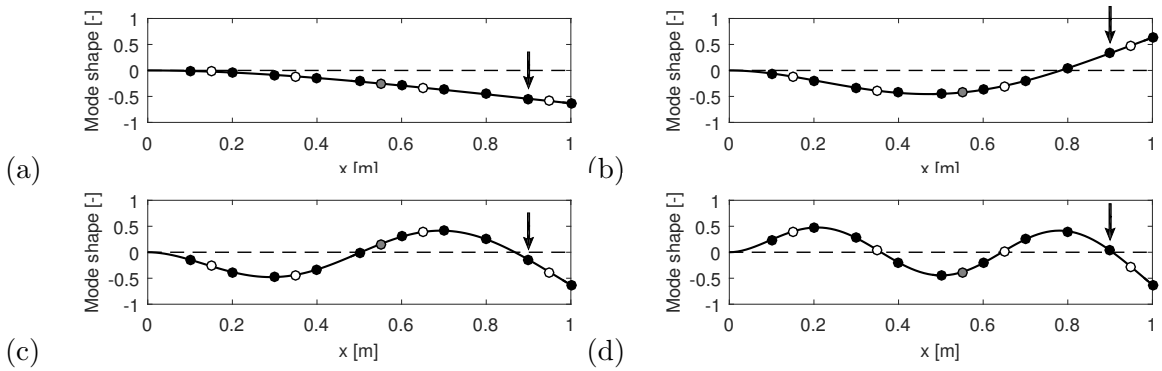

Fig. 2: Mass normalized bending mode shape for (a) mode 1, (b) mode 2, (c) mode 3, and (d) mode 4. The undeformed neutral axis is shown by a black dashed line. The markers indicate the sensor positions (black: accelerometer, white: displacement sensor, gray: location for acceleration estimation). The arrow indicates the force location.

A modally reduced order model of the structure is applied in the numerical simulations. When proportional damping is assumed, the continuous-time decoupled equations of motion are given by:

$$\ddot{\mathbf{z}}(t) + \mathbf{\Gamma}\dot{\mathbf{z}}(t) + \mathbf{\Omega}^2\mathbf{z}(t) = \mathbf{\Phi}^{\mathrm{T}}\left(\mathbf{S}_{\mathrm{p}}(t)\mathbf{p}(t) + \mathbf{S}_{\mathrm{p_S}}(t)\mathbf{p}_{\mathrm{S}}(t)\right) \tag{29}$$

where $\mathbf{z}(t) \in \mathbb{R}^{n_{\mathrm{m}}}$ is the vector of modal coordinates, with n_{m} the number of modes taken into account in the model. The excitation is split in (1) the contribution of forces $\mathbf{p}(t)$ that are to be estimated and (2) the contribution of additional unknown forces $\mathbf{p}_{\mathrm{S}}(t)$. The latter represent for

example the wind loads that are acting on a bridge when estimating the vehicle loads applied to the structure. Both excitation sources are written as the product of a matrix specifying the force locations, $\mathbf{S}_{\mathrm{p}}(t) \in \mathbb{R}^{n_{\mathrm{dof}} \times n_{\mathrm{p}}}$ and $\mathbf{S}_{\mathrm{pS}}(t) \in \mathbb{R}^{n_{\mathrm{dof}} \times n_{\mathrm{pS}}}$, and a time history vector, $\mathbf{p}(t) \in \mathbb{R}^{n_{\mathrm{p}}}$ and $\mathbf{p}_{\mathrm{S}}(t) \in \mathbb{R}^{n_{\mathrm{pS}}}$, with n_{p} the number of forces to be estimated and n_{pS} the number of additional forces (which is generally unknown). The number of degrees of freedom is denoted by n_{dof}. For the remainder of this example, the selection matrix $\mathbf{S}_{\mathrm{p}}(t)$ is assumed to be time-invariant. $\mathbf{\Gamma} \in \mathbb{R}^{n_{\mathrm{m}} \times n_{\mathrm{m}}}$ is a diagonal matrix containing the terms $2\xi_j\omega_j$ on its diagonal, where ω_j and ξ_j are the natural frequency and modal damping ratio corresponding to mode j, respectively. $\mathbf{\Omega} \in \mathbb{R}^{n_{\mathrm{m}} \times n_{\mathrm{m}}}$ is a diagonal matrix as well, containing the natural frequencies ω_j on its diagonal, and $\mathbf{\Phi} \in \mathbb{R}^{n_{\mathrm{dof}} \times n_{\mathrm{m}}}$ is a matrix containing the mass normalized mode shapes $\boldsymbol{\phi}_j$ as columns.

The output vector $\mathbf{d}(t) \in \mathbb{R}^{n_{\mathrm{d}}}$ is written as a combination of acceleration, velocity and displacement or strain measurements:

$$\mathbf{d}(t) = \mathbf{S}_{\mathrm{d,a}}\mathbf{\Phi}\ddot{\mathbf{z}}(t) + \mathbf{S}_{\mathrm{d,v}}\mathbf{\Phi}\dot{\mathbf{z}}(t) + \mathbf{S}_{\mathrm{d,d}}\mathbf{\Phi}\mathbf{z}(t) + \mathbf{v}_{\mathrm{M}[k]} \tag{30}$$

where $\mathbf{S}_{\mathrm{d,a}}$, $\mathbf{S}_{\mathrm{d,v}}$, and $\mathbf{S}_{\mathrm{d,d}} \in \mathbb{R}^{n_{\mathrm{d}} \times n_{\mathrm{dof}}}$ are selection matrices indicating the degrees of freedom corresponding to the acceleration, velocity and displacement or strain measurements, respectively. The vector $\mathbf{v}_{\mathrm{M}[k]} \in \mathbb{R}^{n_{\mathrm{d}}}$ represents the measurement errors.

Eqs. (29) and (30) can be rewritten in state-space form. After time discretization, Eqs. (1) and (2) are obtained. The state vector $\mathbf{x}_{[k]}$ consists of the modal displacements and velocities: $\mathbf{x}_{[k]} = [\mathbf{z}_{[k]}^{\mathrm{T}} \quad \dot{\mathbf{z}}_{[k]}^{\mathrm{T}}]^{\mathrm{T}}$. The state-feedback matrix $\mathbf{A}$ and state-input matrix $\mathbf{B}$ in Eq. (1) are here calculated as:

$$\mathbf{A} = \exp\left(\begin{bmatrix} \mathbf{0} & \mathbf{I}_{n_{\mathrm{m}}} \\ -\mathbf{\Omega}^2 & -\mathbf{\Gamma} \end{bmatrix} \Delta t\right) \tag{31}$$

$$\mathbf{B} = (\mathbf{A} - \mathbf{I}_{n_{\mathrm{s}}}) \begin{bmatrix} \mathbf{0} & \mathbf{I}_{n_{\mathrm{m}}} \\ -\mathbf{\Omega}^2 & -\mathbf{\Gamma} \end{bmatrix}^{-1} \begin{bmatrix} \mathbf{0} \\ \mathbf{\Phi}^{\mathrm{T}}\mathbf{S}_{\mathrm{p}} \end{bmatrix} \tag{32}$$

where $\mathbf{I}_{n_{\mathrm{m}}} \in \mathbb{R}^{n_{\mathrm{m}} \times n_{\mathrm{m}}}$ and $\mathbf{I}_{n_{\mathrm{s}}} \in \mathbb{R}^{n_{\mathrm{s}} \times n_{\mathrm{s}}}$ are identity matrices, with n_{m} the number of modes included in the system model and n_{s} the number of system states ($= 2n_{\mathrm{m}}$), and Δt is the sampling time step. The expressions for $\mathbf{A}$ and $\mathbf{B}$ in Eqs. (31) and (32) are obtained by applying a zero order hold assumption on the input vector $\mathbf{p}_{[k]}$ in the discretization of the system. The reader is referred to [21] for a detailed overview of other common time discretization schemes.

The expressions for the state-output matrix $\mathbf{G}$ and the direct transmission matrix $\mathbf{J}$ in Eq. (2) are independent on the time discretization scheme and are calculated as:

$$\mathbf{G} = \begin{bmatrix} \mathbf{S}_{\mathrm{d,d}}\mathbf{\Phi} - \mathbf{S}_{\mathrm{d,a}}\mathbf{\Phi}\mathbf{\Omega}^2 & \mathbf{S}_{\mathrm{d,v}}\mathbf{\Phi} - \mathbf{S}_{\mathrm{d,a}}\mathbf{\Phi}\mathbf{\Gamma} \end{bmatrix} \tag{33}$$

$$\mathbf{J} = \begin{bmatrix} \mathbf{S}_{\mathrm{d,a}}\mathbf{\Phi}\mathbf{\Phi}^{\mathrm{T}}\mathbf{S}_{\mathrm{p}} \end{bmatrix} \tag{34}$$

In absence of modeling errors, the process noise $\mathbf{w}_{[k]}$ and measurement noise $\mathbf{v}_{[k]}$ account for the unknown excitation and measurement noise and are given by:

$$\mathbf{w}_{[k]} = \mathbf{B}'\mathbf{p}_{\mathrm{S}[k]} \tag{35}$$

$$\mathbf{v}_{[k]} = \mathbf{J}'\mathbf{p}_{\mathrm{S}[k]} + \mathbf{v}_{\mathrm{M}[k]} \tag{36}$$

The matrices $\mathbf{B}' \in \mathbb{R}^{n_\mathrm{s} \times n_\mathrm{pS}}$ and $\mathbf{J}' \in \mathbb{R}^{n_\mathrm{d} \times n_\mathrm{pS}}$ relate the state vector $\mathbf{x}_{[k+1]}$ and the output vector $\mathbf{d}_{[k]}$, respectively, to the vector of stochastic forces $\mathbf{p}_{\mathrm{S}[k]}$ (see also [13]).

The model considered in the numerical simulations is constructed from the first four bending modes of the beam (see Fig. 2). A sampling frequency of 4 kHz is applied in the time discretization. The input $\mathbf{p}_{[k]}$ consists of one vertical force p, applied at a distance of 0.1 m from the free end of the beam (see Fig. 1). The presented smoothing algorithm is applied for the estimation of (1) the vertical force p and (2) the corresponding vertical acceleration a_{11} (see Fig. 1).

3.2. Conditions for invertibility

The conditions which need to be satisfied by the sensor network to allow for system inversion without any time delay ($L = 0$), a.k.a. instantaneous system inversion, have been previously discussed in [16]. A distinction is made between (1) invertibility conditions, (2) stability conditions, and (3) conditions to ensure that a unique solution can be obtained by the system inversion. The invertibility conditions can be relaxed by adopting a time delay $L > 0$, as follows from Theorem 3.1.

Theorem 3.1. *The system described by Eqs.* (1) *and* (2) *can be inverted with a delay L if and only if*

$$\mathrm{rank}\left(\boldsymbol{\mathcal{H}}_L\right) - \mathrm{rank}\left(\boldsymbol{\mathcal{H}}_{L-1}\right) = n_\mathrm{p} \tag{37}$$

where $\mathrm{rank}\left(\boldsymbol{\mathcal{H}}_{-1}\right) = 0$.

Proof. The proof is given by Sain and Massey in [22]. □

It follows directly from Theorem 3.1 that if the system can be inverted with a delay L_0, it can also be inverted with a delay $L \geq L_0$. For $L = 0$ the invertibility condition given in Eq. (37) reduces to the condition presented in [16], i.e. $\mathrm{rank}(\mathbf{J}) = n_\mathrm{p}$. It is proven in [16] that direct invertibility ($L = 0$) requires at least n_p acceleration measurements. The application of a time delay $L > 0$ may allow relaxing the conditions on the minimally required number of accelerations.

As shown in [16] the minimally required number of displacement and/or strain measurements is determined by the stability and uniqueness conditions for system inversion. The stability and uniqueness conditions are system characteristics and therefore do not change with the delay applied in the estimation. Including a time delay in the estimation therefore does not allow reducing the minimally required number of displacement/strain measurements. The reader is referred to [16] for a detailed overview and illustration of the stability and uniqueness conditions.

Although the invertibility condition given in Theorem 3.1 ensures the invertibility of the discrete-time reduced-order model given by Eqs. (1) and (2) for a given delay L, it does not necessarily impose invertibility of the underlying physical structure. Indeed, if the time delay $L\Delta t$ applied in the system inversion is smaller than the wave travel time between the force and response in the real system, the measured response $\mathbf{d}_{L[k]}$ does not contain information on the applied forces $\mathbf{p}_{[k]}$. In this case, the system inversion problem is ill-posed, which can result in large estimation uncertainty (see also [3]).

In the following, a distinction is made between two sensor configurations S_1 and S_2 (see Table 1). Sensor configuration S_1 consists of one acceleration a_9 that is collocated with the estimated force p and one displacement d_4. Sensor configuration S_2 consists of one acceleration a_1 and one displacement d_1, which are both not collocated with the estimated force p.

Configuration	Sensors
S_1	a_9, d_4
S_2	a_1, d_1

Table 1: Overview of the sensor configurations used in the illustration.

The sensor configurations S_1 and S_2 both satisfy the conditions for instantaneous system inversion presented in [16] and therefore allow for system inversion with any delay $L \geq 0$ (Theorem 3.1). The acceleration ensures a direct feedthrough necessary for instantaneous inversion ($L = 0$). For sensor configuration S_1, the acceleration a_9 can be omitted for $L > 0$. It is indeed found that Eq. (37) holds for $L > 0$ when the response consists of a single displacement d_4, meanwhile satisfying the stability and uniqueness conditions. In order to allow for a fair comparison of the results obtained for smoothing ($L > 0$) and filtering ($L = 0$), both the displacement d_4 and acceleration a_{10} are accounted for in the following, however. For sensor configuration S_2, omitting acceleration a_1 leads to unstable transmission zeros and therefore instability of the system inversion [16]. Imposing a time delay $L > 0$ in this case therefore does not allow reducing the sensor configuration.

3.3. Sensor configuration S_1

The smoothing algorithm introduced in Section 2.2 is first applied for the identification of an impact force p and the estimation of the corresponding extrapolated response a_{11} in the case of a collocated acceleration measurement. The impact force is a triangular pulse that increases linearly from zero at time $t = 0.2$ s to 100 N at $t = 0.202$ s, before decreasing linearly to zero at $t = 0.204$ s (see Fig. 4). The system response $\mathbf{d}_{[k]}$ considered in the estimation consists of one acceleration a_9, that is collocated with the estimated force p, and one displacement d_4, see also Fig. 3. It was found in [13] that collocated acceleration measurements generally allow for accurate force and response estimation.

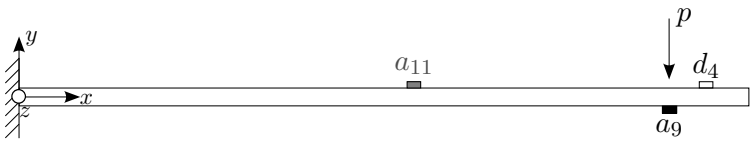

Fig. 3: Force and sensor configuration S_1 (p: force, a_i: accelerometer i, and d_i: displacement sensor i).

Process and measurement noise are introduced by considering stochastic unmodeled forces $\mathbf{p}_{\mathrm{S}[k]}$ that are acting on the structure in addition to the force p that is to be identified. The stochastic forces $\mathbf{p}_{\mathrm{S}[k]}$ consist of ten vertical forces, acting at the location of accelerometers a_1 – a_{10} (see Fig. 1). The time history of each stochastic force is drawn independently from a normal distribution with zero mean value and a standard deviation $\sigma_{\mathrm{p_S}}$ of 0.1 N. The response $\mathbf{d}_{[k]}$ is contaminated by (stochastic) additive measurement errors, that are drawn independently from a normal distribution with zero mean value and a standard deviation of 10^{-6} m and 10^{-2} m/s^2 for the displacement and acceleration measurements, respectively.

For the application of the smoothing algorithm, the initial state vector $\mathbf{x}_{[0|L-1]}$ and its corresponding error covariance matrix $\mathbf{P}_{\mathrm{x}[0|L-1]}$ are both assigned a zero value. The noise covariance

matrices $\mathbf{Q}$, $\mathbf{R}$, and $\mathbf{S}$ in this case correspond to the white noise processes and are calculated as:

$$\begin{bmatrix} \mathbf{Q} & \mathbf{S} \\ \mathbf{S}^{\mathrm{T}} & \mathbf{R} \end{bmatrix} = \begin{bmatrix} \mathbf{B}' \\ \mathbf{J}' \end{bmatrix} \mathbf{C}_{\mathrm{p}} \begin{bmatrix} \mathbf{B}'^{\mathrm{T}} & \mathbf{J}'^{\mathrm{T}} \end{bmatrix} + \begin{bmatrix} \mathbf{0} & \mathbf{0} \\ \mathbf{0} & \mathbf{R}_{\mathrm{M}} \end{bmatrix} \tag{38}$$

where $\mathbf{C}_{\mathrm{p}} \in \mathbb{R}^{n_{\mathrm{pS}} \times n_{\mathrm{pS}}}$ is the covariance matrix of the stochastic forces $\mathbf{p}_{\mathrm{S}[k]}$, which equals $\sigma^2_{\mathrm{p_S}} \mathbf{I}_{n_{\mathrm{pS}}}$ for the case of n_{pS} independent stochastic forces with standard deviation $\sigma_{\mathrm{p_S}}$, as considered in this example. The measurement error covariance matrix $\mathbf{R}_{\mathrm{M}} \in \mathbb{R}^{n_{\mathrm{d}} \times n_{\mathrm{d}}}$ is diagonal with the variance of the measurement errors on its diagonal, i.e. 10^{-12} m^2 and 10^{-4} (m/s^2)^2 for the displacement and acceleration measurements, respectively. The noise covariance matrices $\mathbf{R}_{\mathrm{e}}$, $\mathbf{R}_{\mathrm{c}}$, and $\mathbf{S}_{\mathrm{c}}$ are similarly obtained as:

$$\mathbf{R}_{\mathrm{e}} = \mathbf{J}'_{\mathrm{e}} \mathbf{C}_{\mathrm{p}} \mathbf{J}'^{\mathrm{T}}_{\mathrm{e}}, \quad \mathbf{R}_{\mathrm{c}} = \mathbf{J}'_{\mathrm{e}} \mathbf{C}_{\mathrm{p}} \mathbf{J}'^{\mathrm{T}}, \quad \mathbf{S}_{\mathrm{c}} = \mathbf{J}'_{\mathrm{e}} \mathbf{C}_{\mathrm{p}} \mathbf{B}'^{\mathrm{T}} \tag{39}$$

where the matrix $\mathbf{J}'_{\mathrm{e}}$ relates the vector of extrapolated output quantities $\mathbf{d}_{\mathrm{e}[k]}$ to the vector of stochastic forces $\mathbf{p}_{\mathrm{S}[k]}$.

It is noted that the so-called noise covariance matrices adopted in the estimation must not necessarily agree with the true noise covariance, as is the case here (see also Section 4). Any other value of these matrices can be applied but results in a different estimation uncertainty. The error covariance matrices $\mathbf{P}_{\mathrm{p}[k|k+L]}$, $\mathbf{P}_{\mathrm{x}[k|k+L-1]}$, and $\mathbf{P}_{\mathrm{d_e}[k|k+L]}$ only represent the actual error on the estimated quantities when the noise covariance matrices represent the actual noise covariance. For any choice of the noise covariance matrices, the estimation errors can be quantified by means of the uncertainty quantification approach presented in [13], that can be readily extended for the smoothing algorithm presented in this paper. This approach also allows to distinguish between the uncertainty introduced by (1) measurement noise and (2) unmodeled stochastic excitation, as illustrated hereafter.

In the following, the smoothing algorithm is first applied for a time delay $L = 5$ to verify the correct implementation of the algorithm. Next, a sensitivity analysis is performed to investigate how the estimation uncertainty introduced by the noise processes changes with the time delay L.

Fig. 4 compares the estimated force obtained from the smoothing algorithm for $L = 5$ to the applied impact force. Fig. 5 compares the estimated acceleration $\hat{a}_{11}$ (for $L = 5$) to the actual acceleration as obtained from a forward time domain calculation. A very good agreement between the time history of the actual and estimated quantities is observed. Small errors remain, however, as seen from the frequency spectra. These errors are due to the noise processes, i.e. the measurement noise and stochastic excitation. Fig. 6 shows the evolution of the diagonal value of the error covariance matrices $\mathbf{P}_{\mathrm{p}[k|k+L]}$ and $\mathbf{P}_{\mathrm{d_e}[k|k+L]}$ over time, representing the error variance of the estimated force $\hat{p}$ and the estimated acceleration $\hat{a}_{11}$, respectively. The error variance evolves towards a steady-state value, which depends on the noise statistics $\mathbf{Q}$, $\mathbf{R}$, and $\mathbf{S}$, as well as on the sensor configuration. Only a low number of time steps is required to reach the steady state values. In the case of white noise, the error covariance matrices $\mathbf{P}_{\mathrm{p}[k|k+L]}$ and $\mathbf{P}_{\mathrm{d_e}[k|k+L]}$ represent the covariance of the error on the estimated quantities. It is indeed found that the error on the estimated force $\hat{p}$ and acceleration $\hat{a}_{11}$ has a variance of 0.052 N^2 and 0.027 (m/s^2)^2, respectively, which corresponds to the steady-state values observed in Figs. 6a and 6b, respectively.

Fig. 7 shows the error variance on the estimated force $\hat{p}$ and the estimated acceleration $\hat{a}_{11}$ as a function of the time delay L adopted for smoothing. The error variance is obtained from the steady-state error covariance matrices $\mathbf{P}_{\mathrm{p}[k|k+L]}$ and $\mathbf{P}_{\mathrm{d_e}[k|k+L]}$, as discussed previously. The error variance can be decomposed in its contributions due to measurement noise and unknown

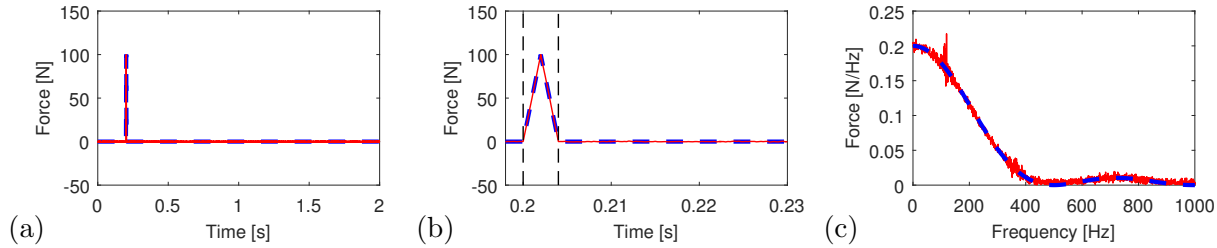

Fig. 4: (a) Time history, (b) detail time history, and (c) amplitude of the narrow band frequency spectrum of the applied impact force (black dashed line) and the estimated force (gray solid line, $L = 5$) for **sensor configuration $\boldsymbol{S_1}$**. The begin and end of the impact are indicated in (b) by a vertical dashed line.

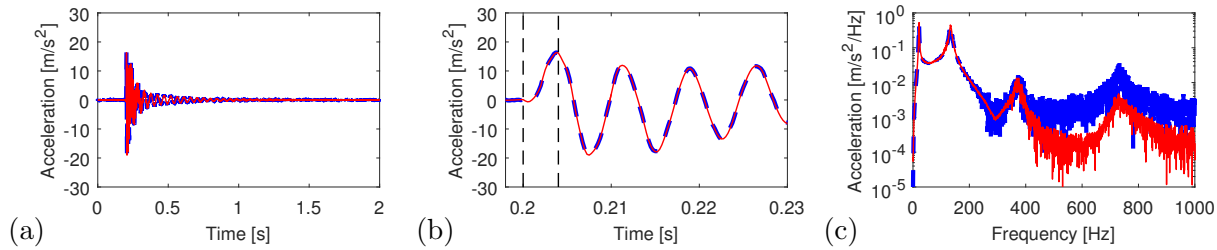

Fig. 5: (a) Time history, (b) detail time history, and (c) amplitude of the narrow band frequency spectrum of the actual acceleration a_{11} (black dashed line) and the estimated acceleration (gray solid line, $L = 5$) for **sensor configuration $\boldsymbol{S_1}$**. The begin and end of the impact are indicated in (b) by a vertical dashed line.

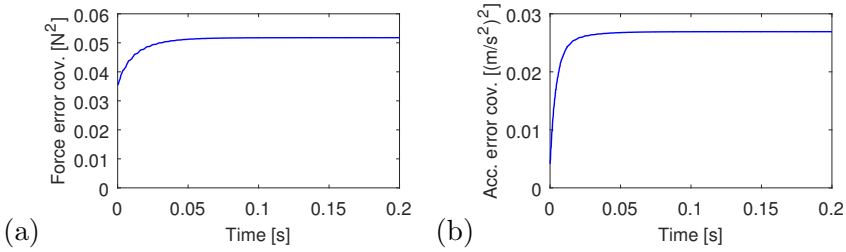

Fig. 6: Evolution of (a) the error variance of the estimated force $\hat{p}$ and (b) the error variance of the estimated acceleration $\hat{a}_{11}$ with time for $L = 5$ (**sensor configuration $\boldsymbol{S_1}$**).

stochastic forces following the uncertainty quantification approach presented in [13]. It is observed from Fig. 7 that for this case of a collocated acceleration measurement the estimation errors on both the estimated force and acceleration are mainly originating from the unknown stochastic excitation. The contribution of the measurement noise to the estimation errors is small, as the direct feedthrough from the force p to the collocated acceleration a_9 makes the estimation less sensitive to measurement noise (see also [13]). The large direct feedthrough is observed from the impulse response in Fig. 8, which shows the acceleration a_9 due to a unit impulse force ($p_{[0]} = 1$ N, $p_{[k]} = 0$ N for $k > 0$). As the instantaneous response is far more informative than the response at future time steps, the algorithm in the system inversion mainly relies on the instantaneous response (at time step k) and only a very small weight is assigned to the response at time steps $k + 1$ to $k + L$. As a result, no significant dependence of the error variance on the time delay L is observed.

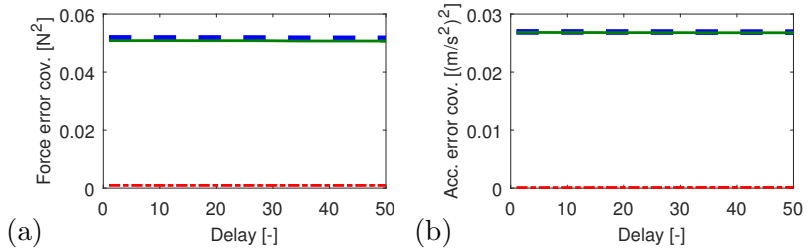

Fig. 7: Error variance of (a) the estimated force $\hat{p}$ and (b) the estimated acceleration $\hat{a}_{11}$ as a function of the time delay L for **sensor configuration S_1** (blue dashed line). The error variance due to measurement noise and unmodeled stochastic forces is given by a red dash-dotted line and a green solid line, respectively.

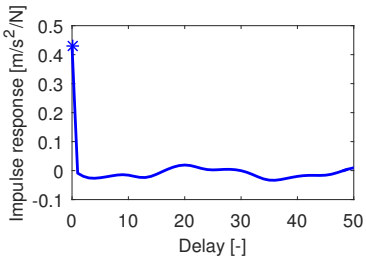

Fig. 8: Impulse response for acceleration a_9 and force p.

3.4. Sensor configuration S_2

It was found in [13] that sensor configurations which do not include collocated acceleration measurements can result in a very high sensitivity to measurement noise. It is therefore investigated in this subsection how the error variance changes with the delay L for the case of non-collocated response measurements. The system response considered in the estimation consists of one acceleration a_1 and one displacement d_1, that are both non-collocated with the estimated force p (see also Fig. 9).

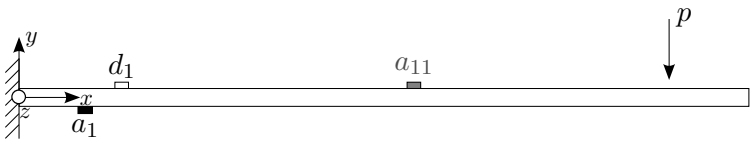

Fig. 9: Force and sensor configuration S_2 (p: force, a_i: accelerometer i, and d_i: displacement sensor i).

The same process and measurement noise are considered as in Section 3.3, i.e. ten independent zero mean Gaussian white stochastic forces with a standard deviation $\sigma_{\mathrm{p_S}}$ of 0.1 N are acting on the beam and zero mean Gaussian white measurement noise is applied with a standard deviation of 10^{-6} m and 10^{-2} m/s^2 for the displacement and acceleration measurements, respectively. The noise covariance matrices $\mathbf{Q}$, $\mathbf{R}$, $\mathbf{S}$, $\mathbf{R}_{\mathrm{e}}$, $\mathbf{R}_{\mathrm{c}}$, and $\mathbf{S}_{\mathrm{c}}$ assumed for smoothing are obtained from Eqs. (38) and (39).

Fig. 10 shows the error variance on the estimated force $\hat{p}$ and the estimated acceleration $\hat{a}_{11}$ as a function of the time delay L adopted for smoothing in the case of non-collocated response measurements. As for sensor configuration S_1, the individual contributions of the measurement noise and the unknown stochastic forces to the error variance is shown. In addition, a comparison is made with the (total) error variance obtained in case of filtering ($L = 0$) for both sensor

configurations. As opposed to the case of collocated measurements (Fig. 7), the error variance for non-collocated measurements is significantly affected by the delay L adopted for smoothing. This mainly holds for the contribution of the measurement noise, which dominates the estimation errors for a time delay L up to about 30. It is observed from the impulse response for acceleration a_1 in Fig. 11 that for this case of a non-collocated acceleration measurement the direct feedthrough is of comparable magnitude as the response at future time steps. Taking into account the response at future time steps $k+1$ to $k+L$ therefore makes the estimation less sensitive to measurement noise with respect to filtering ($L = 0$). The contribution of the error variance due to the unmodeled stochastic forces also depends on the weighing of the data, as observed from Fig. 10. Note that this contribution is not monotonically decreasing with the time delay L, as opposed to the contribution of the measurement noise (Fig. 10a). Through the choice of the gain matrices, the smoothing algorithm minimizes the total error variance of the estimated quantities, including both the contributions of measurement noise and unknown stochastic forces. Although the total estimation error decreases as more data is used in the estimation (i.e. with increasing L), the individual components do not necessarily show a monotonic decrease.

For large values of L, the error variance of the estimated force $\hat{p}$ (Fig. 10a, $\mathbf{P}_{\mathrm{p}[k|k+L]} = 5.56\ \mathrm{N}^2$) is still significantly larger than the error variance obtained for filtering in case of collocated acceleration measurements ($\mathbf{P}_{\mathrm{p}[k|k]} = 0.052\ \mathrm{N}^2$). For the acceleration $\hat{a}_{11}$, however, the application of a large time delay $L \geq 30$ in this example results in more accurate response estimates as compared to sensor configuration S_1 (see Fig. 10b). This conclusion cannot be generalized and is case-specific. As will be discussed in the next subsection, filtering ($L = 0$) requires a much smaller calculation time and should therefore be preferred when collocated measurements are available. When collocated measurements cannot be performed, however, the application of a delay in the estimation can significantly reduce the estimation uncertainty introduced by the noise processes.

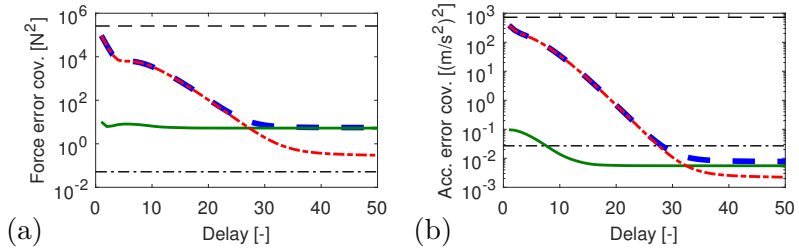

Fig. 10: Error variance of (a) the estimated force $\hat{p}$ and (b) the estimated acceleration $\hat{a}_{11}$ as a function of the time delay L for **sensor configuration S_2** (blue dashed line). The error variance due to measurement noise and unmodeled stochastic forces is given by a red dash-dotted line and a green solid line, respectively. The error variance obtained for filtering ($L = 0$) is indicated by a black dashed line (sensor configuration S_2) and a black dash-dotted line (sensor configuration S_1).

3.5. Computational cost

This section investigates how the calculation time of the smoothing algorithm changes with the time delay L. Fig. 12a shows the average calculation time for one time step $\bar{T}_{\mathrm{c}}(L)$ as a function of the time delay L. The calculation includes the evaluation of Eqs. (9) to (18). The additional response estimation step in Eq. (22) is not included in the comparison, since it is computationally inexpensive ($\bar{T}_{\mathrm{c}} = \pm 10^{-5}$ ms) and independent of the time delay L. The calculations have been performed in MATLAB using an Intel® Core™ i7-2720QM 2.20GHz CPU. The calculation time

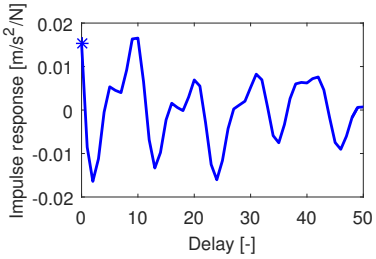

Fig. 11: Impulse response for acceleration a_1 and force p.

$\bar{T}_c(L)$ is obtained by averaging over 8000 time steps. As in the previous sections, a comparison is made to filtering ($L = 0$). It is observed from Fig. 12a that the calculation time significantly increases with the adopted time delay L. Even more, the smoothing algorithm for the presented example cannot be applied in real time since $\bar{T}_c(L) > \Delta t = 0.25$ ms, where Δt is the sampling time step.

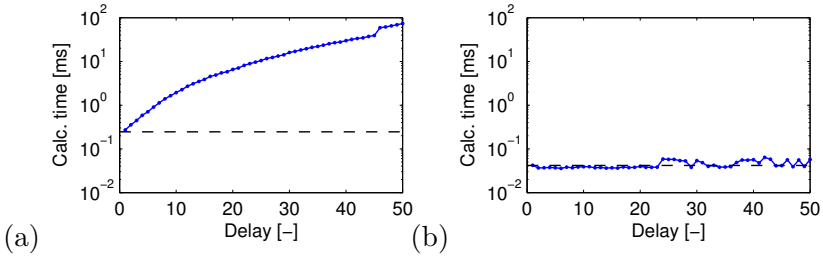

Fig. 12: Calculation time $\bar{T}_c(L)$ as a function of the time delay L (a) for the original smoothing algorithm and (b) with steady-state initialization. The calculation time for filtering ($L = 0$) is indicated by a black dashed line.

On the condition that the smoothing algorithm is stable (see Section 3.2), the error covariance matrices $\mathbf{P}_{\mathrm{p}[k|k+L]}$ and $\mathbf{P}_{\mathrm{x}[k+1|k+L]}$, as well as the gain matrices $\mathbf{M}_{L[k]}$ and $\mathbf{K}_{L[k]}$ evolve towards a steady-state value as the algorithm proceeds in time. The steady-state value of the matrices depends on the noise covariance matrices $\mathbf{Q}$, $\mathbf{R}$, and $\mathbf{S}$, on the forces to be estimated, as well as on the sensor configuration. As illustrated in Fig. 6, only a low number of time steps is required to reach the steady state. Since the calculation of the gain matrices $\mathbf{M}_{L[k]}$ and $\mathbf{K}_{L[k]}$ is computationally very expensive, one could pre-compute the steady-state value of these matrices, before their continuous application in the input and state estimation step over time, i.e. Eqs. (13) and (18), respectively. By applying a steady-state initialization of the algorithm, the calculation time is significantly reduced and becomes nearly independent on the time delay L, as evidenced by Fig. 12b. For every time delay considered, the calculation time $\bar{T}_c(L)$ is much smaller than the sampling time step $\Delta t = 0.25$ ms, enabling real-time joint input-state estimation even for large values of the delay L.

In the steady-state initialization, the convergence towards the steady-state is checked by means of the convergence rate $R_{\mathrm{ss}[k]}$, that is defined as follows:

$$R_{\mathrm{ss}[k]} = \frac{\mathrm{tr}\left(\left|\mathbf{P}_{\mathrm{p}[k|k+L]} - \mathbf{P}_{\mathrm{p}[k-1|k+L-1]}\right|\right)}{\mathrm{tr}\left(\mathbf{P}_{\mathrm{p}[k|k+L]}\right)} \tag{40}$$

where $|\cdot|$ returns the absolute value of all elements in a matrix. It is assumed that steady-state is reached when $R_{\mathrm{ss}[k]} < 10^{-6}$.

4. Experimental validation

The structure under consideration in the validation study is a footbridge, located in Ninove (Belgium). The two-span cable-stayed steel bridge, shown in Fig. 13, has a main and secondary span of 36 m and 22.5 m, respectively.

Fig. 13: The footbridge in Ninove, Belgium.

The structure is excited by a sequence of hammer impacts, applied vertically on the bridge deck. The sensor configuration is shown in Fig. 14. The acceleration response of the footbridge has been recorded in three orthogonal directions at 12 locations on the bridge deck, using 12 wireless GeoSIG GMS-18 units. In addition, a National Instruments (NI) PXI data acquisition system has been used to record (1) the vertical acceleration at nodes 27 and 48, obtained from PCB 393B04 uniaxial accelerometers, (2) the vertical displacement of the bridge deck at nodes 27 and 40, obtained from AWLG 008M optical displacement sensors, and (3) the impact loads applied vertically at nodes 27 and 48 using PCB 086D50 instrumented hammers (mass 5.5 kg).

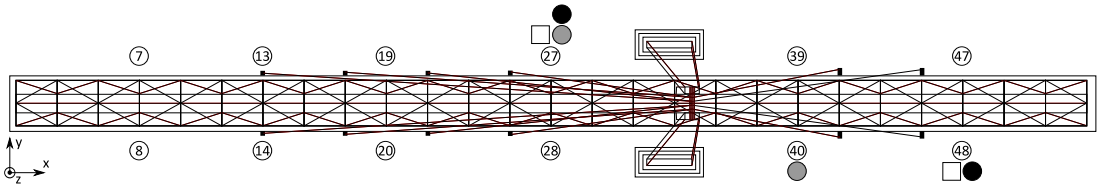

Fig. 14: Sensor configuration Ninove footbridge (white circle: GMS-18 unit, black circle: uniaxial accelerometer, gray circle: optical displacement sensor, white square: instrumented hammer).

The measured response and force signals used in the analysis are all digitally lowpass filtered by means of an eighth-order Chebyshev type I lowpass filter with a cutoff frequency of 16 Hz, in both the forward and the reverse direction to remove all phase distortion, and then re-sampled at 40 Hz. Next, the acceleration signals obtained from the NI system and the GMS-18 units are additionally digitally highpass filtered by means of a fifth order Butterworth filter with a cutoff frequency of 0.5 Hz and 0.1 Hz, respectively, in both the forward and the reverse direction. The aim of the filter is to remove the low frequency components from the signals that are contaminated by measurement noise. Finally, a detrend operation is applied to all acceleration signals to remove the (physically meaningless) DC component. The measured displacement signals are relative to the displacements at the start of the experiment.

The force identification is based on a state-space description of the system, given by equations (1) and (2). The system model used in the present analysis is based on a detailed finite element (FE) model of the structure, that is built using the FE program ANSYS. The reader is referred to [23] for a detailed description of the FE model and the calibration of the model based on the experimental modal parameters that have been obtained through operational modal analysis

(OMA). A reduced-order discrete-time state-space model is constructed from the first 18 modes of the bridge deck, i.e. all modes with a natural frequency that falls within the frequency range 0 Hz to 20 Hz. For each mode, the mass-normalized mode shape of the FE model is used. The natural frequency and modal damping ratio are taken as the experimentally identified values. A zero order hold assumption is applied on the input vector $\mathbf{p}_{[k]}$ in the time discretization.

The remainder of this section shows a comparison of filtering ($L = 0$) and smoothing ($L > 0$) for the identification of impact forces applied vertically to the bridge deck at nodes 27 and 48. It was shown in [23] that the application of acceleration measurements that are collocated with the applied forces allows for accurate reconstruction of the impact forces applied to the bridge deck. The sensor configuration considered in this paper consists of two vertical displacements at nodes 27 and 40 and two vertical accelerations at nodes 7 and 8, measured at a large distance from the forces at nodes 27 and 48.

The noise covariance matrices $\mathbf{Q}$, $\mathbf{R}$, and $\mathbf{S}$ used in the estimation are based on the PSD of the unknown stochastic excitation, that has been estimated from the response of the structure under ambient loading (see also [23]), and the noise characteristics of the sensors. The initial state estimate vector $\mathbf{x}_{[0|L-1]}$ and its error covariance matrix $\mathbf{P}_{[0|L-1]}$ are both assumed zero. A digital highpass filter with a cutoff frequency of 0.2 Hz is applied to the estimated force signals in order to remove low frequency force components that compensate for wind loads.

Fig. 15 shows the results obtained by filtering ($L = 0$). A large discrepancy between the measured and estimated forces is observed. The large estimation uncertainty stems from the ill-posedness of the force identification problem, since the non-collocated response measurements are not instantaneously affected by the system input. Three time intervals can be distinguished for a single impact; (1) the actual impact, (2) the free vibration right after the impact, and (3) ambient vibration. During the impact, the broad band hammer force excites the entire frequency range considered. During the subsequent free vibration phase, the structure vibrates at its natural frequencies and modeling errors result in errors on the estimated forces that generally decay exponentially over time. After the free vibration phase, the measured response is predominantly due to ambient loads, mainly consisting of wind loads in this case. During this phase, the errors on the estimated forces originate from ambient excitation and measurement noise. As found in [13], sensor configurations which do not include collocated acceleration measurements can result in a very high sensitivity to noise, leading to large errors in the force estimation as observed here. The largest estimation errors are obtained for the force applied at node 48. In this case, modeling errors are caused by small errors on the modal properties of the structure and the contribution of out-of-band modes, which have not been accounted for in the model. These modeling errors are the cause of a clear free vibration phase as observed from the time history in Figs. 15a and 15d.

Fig. 16 shows the results obtained by smoothing, assuming a time delay $L = 30$. The estimation errors during the ambient vibration phase and the free vibration phase are significantly lower than those obtained for filtering ($L = 0$, Fig. 15). Although a reasonably good estimate of the forces is obtained, the estimation errors are larger than in the case of collocated measurements (see [23]). Even more, modeling errors prohibit a proper distinction between the two forces, as seen from the spurious peaks in the estimated force at node 48 occuring when an impact force is applied at node 27 (see Fig. 16e).

Fig. 17 shows the error variance of the estimated forces as a function of the time delay L adopted for smoothing. This error variance accounts for measurement noise and unmodeled stochastic forces and is calculated by means of the uncertainty quantification approach presented in [13]. For the case

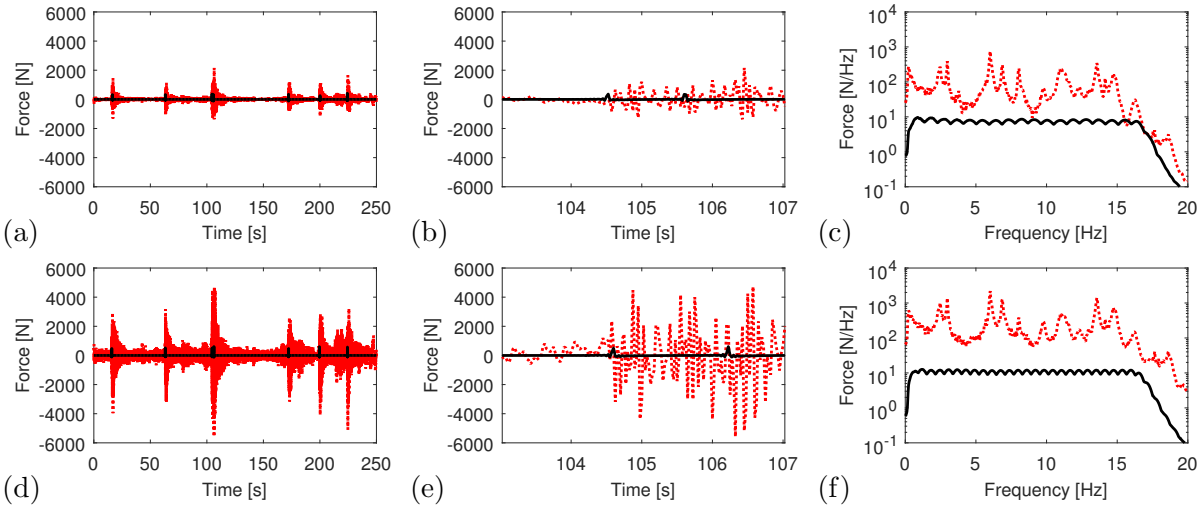

Fig. 15: Time history (left), detail of the time history (middle), and averaged amplitude of the narrow band frequency spectrum (right) of the hammer forces applied at node 27 ((a) – (c)) and node 48 ((d) – (f)) for $\boldsymbol{L = 0}$ **(filtering)**. The measured force signals are shown by a solid black line, the identified force signals by a dotted red line.

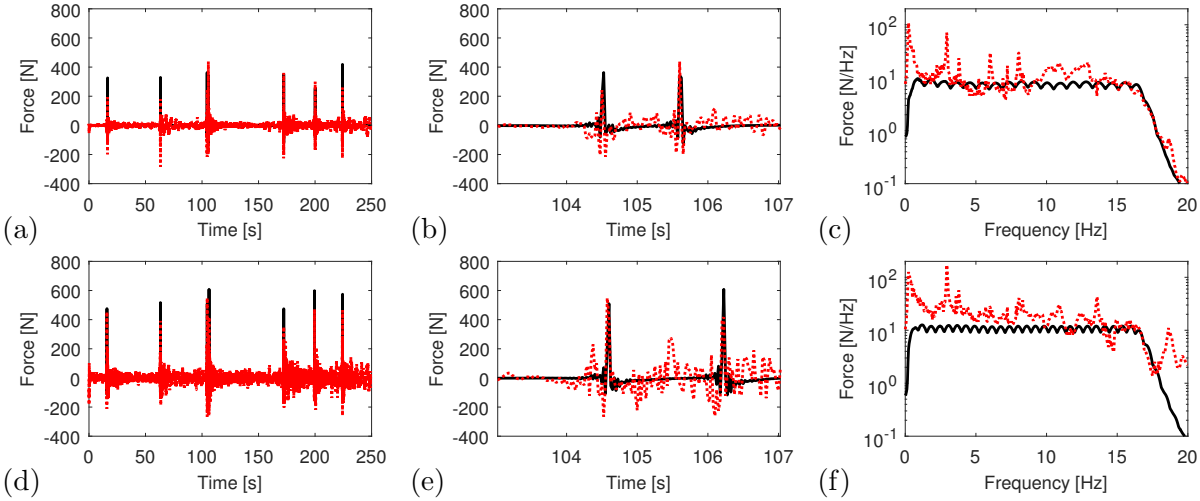

Fig. 16: Time history (left), detail of the time history (middle), and averaged amplitude of the narrow band frequency spectrum (right) of the hammer forces applied at node 27 ((a) – (c)) and node 48 ((d) – (f)) for $\boldsymbol{L = 30}$ **(smoothing)**. The measured force signals are shown by a solid black line, the identified force signals by a dotted red line.

of non-collocated measurements, it is found that the force error variance is significantly affected by the delay L adopted for smoothing. This mainly holds for a time delay L up to about 30. Further increasing the delay does not significantly affect the results.

5. Conclusions

This paper presents a recursive smoothing algorithm where a time delay is assumed for joint input-state estimation. The algorithm can be applied for force identification and response estimation when the dynamic behavior of the structure is adequately represented by a linear model. An illustration for a cantilever steel beam shows that assuming a time delay in the estimation can

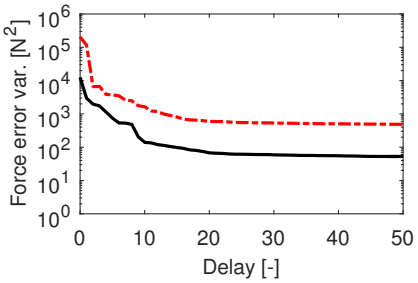

Fig. 17: Error variance of the estimated force at node 27 (solid black line) and node 48 (dash-dotted red line) in the frequency interval from 0.2 Hz to 16 Hz as a function of the delay L.

lead to a significant reduction of the estimation uncertainty introduced by measurement noise, in particular when the response measurements are not collocated with the estimated forces. When the calculation of the gain matrices is included in the recursive estimation, the smoothing process becomes very time-consuming, even for very small values of the time delay. The calculation time of the algorithm can be significantly reduced, however, by pre-computing the steady-state gain matrices. A validation study based on data obtained from a field test on a footbridge confirms the need for a time delay to reduce estimation errors in case of non-collocated response measurements, but also demonstrates that an accurate dynamic model of the structure is essential for accurate force identification.

Acknowledgements

Kristof Maes is a postdoctoral fellow of KU Leuven. The financial support by KU Leuven is gratefully acknowledged. The authors affiliated to KU Leuven are all members of the KU Leuven – BOF PFV/10/002 OPTEC – Optimization in Engineering Center.

Appendix A. Smoothing algorithm for joint input-state estimation

The system under consideration is described by the following linear discrete-time combined deterministic-stochastic state-space description:

$$\mathbf{x}_{[k+1]} = \mathbf{A}\mathbf{x}_{[k]} + \mathbf{B}\mathbf{p}_{[k]} + \mathbf{w}_{[k]} \tag{A.1}$$

$$\mathbf{d}_{[k]} = \mathbf{G}\mathbf{x}_{[k]} + \mathbf{J}\mathbf{p}_{[k]} + \mathbf{v}_{[k]} \tag{A.2}$$

where $\mathbf{x}_{[k]} \in \mathbb{R}^{n_\mathrm{s}}$ is the state vector, $\mathbf{d}_{[k]} \in \mathbb{R}^{n_\mathrm{d}}$ is the measured output vector, and $\mathbf{p}_{[k]} \in \mathbb{R}^{n_\mathrm{p}}$ is the input vector, to be estimated. The system matrices $\mathbf{A}$, $\mathbf{B}$, $\mathbf{G}$, and $\mathbf{J}$ are assumed known. As derived in Section 2.1, the response over $L+1$ consecutive time steps $\mathbf{d}_{L[k]}$, defined in Eq. (3), is given by:

$$\mathbf{d}_{L[k]} = \boldsymbol{\mathcal{O}}_L \mathbf{x}_{[k]} + \boldsymbol{\mathcal{H}}_L \mathbf{p}_{L[k]} + \boldsymbol{\mathcal{N}}_L \mathbf{w}_{L-1[k]} + \mathbf{v}_{L[k]} \tag{A.3}$$

The extended observability matrix $\boldsymbol{\mathcal{O}}_L \in \mathbb{R}^{(L+1)n_\mathrm{d} \times n_\mathrm{s}}$, the Toeplitz matrix $\boldsymbol{\mathcal{H}}_L \in \mathbb{R}^{(L+1)n_\mathrm{d} \times (L+1)n_\mathrm{p}}$, and the matrix $\boldsymbol{\mathcal{N}}_L \in \mathbb{R}^{(L+1)n_\mathrm{d} \times Ln_\mathrm{s}}$ are defined in Eqs. (5) and (6).

In the derivation of the smoothing algorithm, the process noise vector $\mathbf{w}_{[k]} \in \mathbb{R}^{n_\mathrm{s}}$ and measurement noise vector $\mathbf{v}_{[k]} \in \mathbb{R}^{n_\mathrm{d}}$ are assumed to be zero mean and white, with known covariance matrices $\mathbf{Q}$, $\mathbf{R}$, and $\mathbf{S}$, defined by:

$$\mathbb{E}\left[\begin{pmatrix}\mathbf{w}_{[k]}\\ \mathbf{v}_{[k]}\end{pmatrix}\begin{pmatrix}\mathbf{w}_{[l]}^\mathrm{T} & \mathbf{v}_{[l]}^\mathrm{T}\end{pmatrix}\right] = \begin{bmatrix}\mathbf{Q} & \mathbf{S}\\ \mathbf{S}^\mathrm{T} & \mathbf{R}\end{bmatrix}\delta_{[k-l]} \tag{A.4}$$

with $\mathbf{R} > 0$, $\begin{bmatrix}\mathbf{Q} & \mathbf{S}\\ \mathbf{S}^\mathrm{T} & \mathbf{R}\end{bmatrix} \geq 0$, and $\delta_{[k]} = 1$ for $k = 0$ and 0 otherwise.

Finally, it is assumed that an unbiased estimate $\hat{\mathbf{x}}_{[0|L-1]}$ of the initial state is available, with error covariance matrix $\mathbf{P}_{\mathrm{x}[0|L-1]}$ (i.e. $\mathbb{E}[\mathbf{x}_{[0]} - \hat{\mathbf{x}}_{[0|L-1]}] = 0$, $\mathbf{P}_{\mathrm{x}[0|L-1]} = \mathbb{E}[(\mathbf{x}_{[0]} - \hat{\mathbf{x}}_{[0|L-1]})(\mathbf{x}_{[0]}^\mathrm{T} - \hat{\mathbf{x}}_{[0|L-1]}^\mathrm{T})]$). In addition, the estimate $\hat{\mathbf{x}}_{[0|L-1]}$ is assumed independent of the noise processes $\mathbf{w}_{[k]}$ and $\mathbf{v}_{[k]}$ for all k.

The smoothing algorithm estimates the system states $\mathbf{x}_{[k]}$ and the forces $\mathbf{p}_{[k]}$ from a set of response measurements $\mathbf{d}_{[k]}$ obtained at $L+1$ consecutive time steps (i.e. from the response vector $\mathbf{d}_{L[k]}$). A state estimate $\hat{\mathbf{x}}_{[k|l]}$ is defined as an estimate of $\mathbf{x}_{[k]}$, given the output sequence $\mathbf{d}_{[n]}$, with $n = 0, 1, \ldots, l$. An input estimate $\hat{\mathbf{p}}_{[k|l]}$ is defined similarly.

Consider the following two-step recursive smoothing algorithm:

$$\hat{\mathbf{p}}_{[k|k+L]} = \mathbf{M}_{L[k]}\left(\mathbf{d}_{L[k]} - \boldsymbol{\mathcal{O}}_L\hat{\mathbf{x}}_{[k|k+L-1]}\right) \tag{A.5}$$

$$\hat{\mathbf{x}}_{[k+1|k+L]} = \mathbf{A}\hat{\mathbf{x}}_{[k|k+L-1]} + \mathbf{K}_{L[k]}(\mathbf{d}_{L[k]} - \boldsymbol{\mathcal{O}}_L\hat{\mathbf{x}}_{[k|k+L-1]}) \tag{A.6}$$

The first step in Eq. (A.5), hereafter referred to as the "input estimation step", yields an estimate of the unknown input vector $\mathbf{p}_{[k]}$, given the measured output up to time step $k+L$. The second step in Eq. (A.6), referred to as the "state estimation step", yields an estimate of the state vector $\mathbf{x}_{[k+1]}$, given the measured output up to time step $k+L$. The gain matrices $\mathbf{M}_{L[k]} \in \mathbb{R}^{n_\mathrm{p} \times (L+1)n_\mathrm{d}}$ and $\mathbf{K}_{L[k]} \in \mathbb{R}^{n_\mathrm{s} \times (L+1)n_\mathrm{d}}$ are determined such that both the input estimates $\hat{\mathbf{p}}_{[k|k+L]}$ and the state estimates $\hat{\mathbf{x}}_{[k+1|k+L]}$ are minimum variance and unbiased (MVU). The calculation of the gain matrices is discussed in the following sections.

Appendix A.1. Input estimation

The input estimation step is given by Eq. (A.5). First, it is checked what condition the gain matrix $\mathbf{M}_{L[k]}$ should satisfy for unbiased input estimation. Combination of Eqs. (A.3) and (A.5) yields the error on the input estimate $\hat{\mathbf{p}}_{[k|k+L]}$, denoted by $\tilde{\mathbf{p}}_{[k|k+L]}$:

$$\begin{aligned}\tilde{\mathbf{p}}_{[k|k+L]} &\triangleq \mathbf{p}_{[k]} - \hat{\mathbf{p}}_{[k|k+L]}\\ &= \left(\breve{\mathbf{I}}_{n_\mathrm{p}} - \mathbf{M}_{L[k]}\boldsymbol{\mathcal{H}}_L\right)\mathbf{p}_{L[k]} - \mathbf{M}_{L[k]}(\boldsymbol{\mathcal{O}}_L\tilde{\mathbf{x}}_{[k|k+L-1]} + \boldsymbol{\mathcal{N}}_L\mathbf{w}_{L-1[k]} + \mathbf{v}_{L[k]})\end{aligned} \tag{A.7}$$

with $\breve{\mathbf{I}}_{n_\mathrm{p}} = [\mathbf{I}_{n_\mathrm{p}} \quad \mathbf{0} \quad \ldots \quad \mathbf{0}] \in \mathbb{R}^{n_\mathrm{p} \times (L+1)n_\mathrm{p}}$, where $\mathbf{I}_{n_\mathrm{p}} \in \mathbb{R}^{n_\mathrm{p} \times n_\mathrm{p}}$ denotes an identity matrix. Let the state estimate $\hat{\mathbf{x}}_{[k|k+L-1]}$ be unbiased, then it follows immediately from Eq. (A.7) that the estimator (A.5) is unbiased for all possible $\mathbf{p}_{L[k]}$ if the following equality holds:

$$\breve{\mathbf{I}}_{n_\mathrm{p}} = \mathbf{M}_{L[k]}\boldsymbol{\mathcal{H}}_L \tag{A.8}$$

Assuming in addition that the initial state estimate $\hat{\mathbf{x}}_{[0|L-1]}$ is unbiased and independent of the noise processes $\mathbf{w}_{[k]}$ and $\mathbf{v}_{[k]}$ for all k, and assuming the noise processes zero mean and white, with noise covariance matrices $\mathbf{Q}$, $\mathbf{R}$, and $\mathbf{S}$, given by Eq. (A.4), the covariance matrix of the error on the input estimate $\hat{\mathbf{p}}_{[k|k+L]}$ is given by:

$$\mathbf{P}_{\mathrm{p}[k|k+L]} \triangleq \mathbb{E}\left[\tilde{\mathbf{p}}_{[k|k+L]}\tilde{\mathbf{p}}_{[k|k+L]}^{\mathrm{T}}\right] = \mathbf{M}_{L[k]}\bar{\mathbf{R}}_{[k]}\mathbf{M}_{L[k]}^{\mathrm{T}} \tag{A.9}$$

where

$$\begin{aligned}\bar{\mathbf{R}}_{[k]} = {} & \boldsymbol{\mathcal{O}}_L\mathbf{P}_{\mathrm{x}[k|k+L-1]}\boldsymbol{\mathcal{O}}_L^{\mathrm{T}} + \mathbf{R}_{L+1}^0 + \boldsymbol{\mathcal{N}}_L\mathbf{Q}_L^0\boldsymbol{\mathcal{N}}_L^{\mathrm{T}} + \boldsymbol{\mathcal{N}}_L\mathbf{S}_L^0 + \mathbf{S}_L^{0^{\mathrm{T}}}\boldsymbol{\mathcal{N}}_L^{\mathrm{T}}\dots \\ & + \boldsymbol{\mathcal{O}}_L\mathbf{P}_{\mathrm{xw}[k]}\boldsymbol{\mathcal{N}}_L^{\mathrm{T}} + \boldsymbol{\mathcal{N}}_L\mathbf{P}_{\mathrm{wx}[k]}\boldsymbol{\mathcal{O}}_L^{\mathrm{T}} + \boldsymbol{\mathcal{O}}_L\mathbf{P}_{\mathrm{xv}[k]} + \mathbf{P}_{\mathrm{vx}[k]}\boldsymbol{\mathcal{O}}_L^{\mathrm{T}}\end{aligned} \tag{A.10}$$

The expression for the state error covariance matrix $\mathbf{P}_{\mathrm{x}[k|k+L-1]}$ $(= \mathbb{E}[\tilde{\mathbf{x}}_{[k|k+L-1]}\tilde{\mathbf{x}}_{[k|k+L-1]}^{\mathrm{T}}])$ is derived in Appendix A.2 (see Eq. (A.23)). The extended noise covariance matrices $\mathbf{Q}_L^i \in \mathbb{R}^{Ln_{\mathrm{s}}\times Ln_{\mathrm{s}}}$, $\mathbf{R}_{L+1}^i \in \mathbb{R}^{(L+1)n_{\mathrm{d}}\times(L+1)n_{\mathrm{d}}}$ and $\mathbf{S}_L^i \in \mathbb{R}^{Ln_{\mathrm{s}}\times(L+1)n_{\mathrm{d}}}$ are defined as:

$$\begin{aligned}\mathbf{Q}_L^i &\triangleq \mathbb{E}\left[\mathbf{w}_{L-1[k-i]}\mathbf{w}_{L-1[k]}^{\mathrm{T}}\right] = \mathrm{diag}_L^i(\mathbf{Q},\mathbf{Q},\dots,\mathbf{Q}) \\ \mathbf{R}_{L+1}^i &\triangleq \mathbb{E}\left[\mathbf{v}_{L[k-i]}\mathbf{v}_{L[k]}^{\mathrm{T}}\right] = \mathrm{diag}_{L+1}^i(\mathbf{R},\mathbf{R},\dots,\mathbf{R}) \\ \mathbf{S}_L^i &\triangleq \mathbb{E}\left[\mathbf{w}_{L-1[k-i]}\mathbf{v}_{L[k]}^{\mathrm{T}}\right] = [\mathrm{diag}_L^i(\mathbf{S},\mathbf{S},\dots,\mathbf{S}),\mathbf{0}] \qquad \text{for } i \geq 0 \\ &\qquad\qquad = [\mathbf{0},\mathrm{diag}_L^{i+1}(\mathbf{S},\mathbf{S},\dots,\mathbf{S})] \qquad \text{for } i < 0\end{aligned} \tag{A.11}$$

where $\mathrm{diag}_j^i(\cdot)$ denotes a block matrix with the j matrices between the brackets on the i-th block diagonal below the main diagonal and zeros elsewhere. The following closed form expressions for the covariance matrices $\mathbf{P}_{\mathrm{xw}[k]}$, $\mathbf{P}_{\mathrm{wx}[k]}$, $\mathbf{P}_{\mathrm{xv}[k]}$, and $\mathbf{P}_{\mathrm{vx}[k]}$ in Eq. (A.10) are obtained:

$$\mathbf{P}_{\mathrm{xw}[k]} = \mathbf{P}_{\mathrm{wx}[k]}^{\mathrm{T}} \triangleq \mathbb{E}\left[\tilde{\mathbf{x}}_{[k|k+L-1]}\mathbf{w}_{L-1[k]}^{\mathrm{T}}\right] \tag{A.12}$$

$$= \sum_{i=1}^{\min(k,L)}\left(\left(\prod_{j=1}^{i-1}\left(\mathbf{A}-\mathbf{K}_{L[k-j]}\boldsymbol{\mathcal{O}}_L\right)\right)\left(\left(\breve{\mathbf{I}}_{n_{\mathrm{s}}}-\mathbf{K}_{L[k-i]}\boldsymbol{\mathcal{N}}_L\right)\mathbf{Q}_L^i - \mathbf{K}_{L[k-i]}\mathbf{S}_L^{-i^{\mathrm{T}}}\right)\right)$$

$$\mathbf{P}_{\mathrm{xv}[k]} = \mathbf{P}_{\mathrm{vx}[k]}^{\mathrm{T}} \triangleq \mathbb{E}\left[\tilde{\mathbf{x}}_{[k|k+L-1]}\mathbf{v}_{L[k]}^{\mathrm{T}}\right] \tag{A.13}$$

$$= \sum_{i=1}^{\min(k,L)}\left(\left(\prod_{j=1}^{i-1}\left(\mathbf{A}-\mathbf{K}_{L[k-j]}\boldsymbol{\mathcal{O}}_L\right)\right)\left(\left(\breve{\mathbf{I}}_{n_{\mathrm{s}}}-\mathbf{K}_{L[k-i]}\boldsymbol{\mathcal{N}}_L\right)\mathbf{S}_L^i - \mathbf{K}_{L[k-i]}\mathbf{R}_{L+1}^i\right)\right)$$

where $\sum_{i=1}^{j}(\cdot) \triangleq \mathbf{0}$ for $i > j$, $\prod_{i=1}^{j}(\cdot) \triangleq \mathbf{I}$ for $i > j$, and $\breve{\mathbf{I}}_{n_{\mathrm{s}}} = [\mathbf{I}_{n_{\mathrm{s}}} \quad \mathbf{0} \quad \dots \quad \mathbf{0}] \in \mathbb{R}^{n_{\mathrm{s}}\times Ln_{\mathrm{s}}}$, with $\mathbf{I}_{n_{\mathrm{s}}} \in \mathbb{R}^{n_{\mathrm{s}}\times n_{\mathrm{s}}}$ an identity matrix.

The gain matrix $\mathbf{M}_{L[k]}$ that yields MVU input estimates is obtained by minimizing the trace of the error covariance matrix $\mathbf{P}_{\mathrm{p}[k+1|k+L]}$ in Eq. (A.9), under the constraint that Eq. (A.8) holds.

In a similar way as for the filtering algorithm in [13], the constraint in Eq. (A.22) is introduced in the optimization problem using Lagrange multipliers. After introduction of the constraint, the optimization problem is written as:

$$\mathbf{M}_{L[k]}^{\star} = \underset{\mathbf{M}_{L[k]} \in \mathbb{R}^{n_\mathrm{p} \times (L+1)n_\mathrm{d}}}{\arg\min} \left(\mathrm{tr} \left\{ \mathbf{M}_{L[k]} \bar{\mathbf{R}}_{[k]} \mathbf{M}_{L[k]}^{\mathrm{T}} \right\} + 2 \ \mathrm{tr} \left\{ (\breve{\mathbf{I}}_{n_\mathrm{p}} - \mathbf{M}_{L[k]} \boldsymbol{\mathcal{H}}_L) \boldsymbol{\Lambda}_{\mathrm{p}[k]}^{\mathrm{T}} \right\} \right) \tag{A.14}$$

where $\boldsymbol{\Lambda}_{\mathrm{p}[k]} \in \mathbb{R}^{n_\mathrm{p} \times (L+1)n_\mathrm{p}}$ is the matrix of Lagrange multipliers. The factor 2 in the second term of the right hand side is introduced for notational convenience. Setting the derivative of the Lagrangian in Eq. (A.14) with respect to $\mathbf{M}_{L[k]}$ and $\boldsymbol{\Lambda}_{\mathrm{p}[k]}$ equal to zero yields respectively:

$$\bar{\mathbf{R}}_{[k]} \mathbf{M}_{L[k]}^{\mathrm{T}} - \boldsymbol{\mathcal{H}}_L \boldsymbol{\Lambda}_{\mathrm{p}[k]}^{\mathrm{T}} = \mathbf{0} \tag{A.15}$$

$$\breve{\mathbf{I}}_{n_\mathrm{p}} = \mathbf{M}_{L[k]} \boldsymbol{\mathcal{H}}_L \tag{A.16}$$

Eqs. (A.15) and (A.16) can be written as a linear system of equations:

$$\begin{bmatrix} \bar{\mathbf{R}}_{[k]} & -\boldsymbol{\mathcal{H}}_L \\ -\boldsymbol{\mathcal{H}}_L^{\mathrm{T}} & \mathbf{0} \end{bmatrix} \begin{bmatrix} \mathbf{M}_{L[k]}^{\mathrm{T}} \\ \boldsymbol{\Lambda}_{\mathrm{p}[k]}^{\mathrm{T}} \end{bmatrix} = \begin{bmatrix} \mathbf{0} \\ -\breve{\mathbf{I}}_{n_\mathrm{p}}^{\mathrm{T}} \end{bmatrix} \tag{A.17}$$

The matrix $\bar{\mathbf{R}}_{[k]} \in \mathbb{R}^{(L+1)n_\mathrm{d} \times (L+1)n_\mathrm{d}}$ is nonsingular. The Hankel matrix $\boldsymbol{\mathcal{H}}_L$ and therefore the Schur complement of the matrix $\bar{\mathbf{R}}_{[k]}$ in the coefficient matrix of Eq. (A.17), i.e. $\boldsymbol{\mathcal{H}}_L^{\mathrm{T}} \bar{\mathbf{R}}_{[k]}^{-1} \boldsymbol{\mathcal{H}}_L \in \mathbb{R}^{(L+1)n_\mathrm{p} \times (L+1)n_\mathrm{p}}$, are not necessarily of full rank $(L+1)n_\mathrm{p}$. If the invertibility conditions presented in Section 3.2 are satisfied, however, the linear system of equations in Eq. (A.17) can be solved for the gain matrix $\mathbf{M}_{L[k]}$ using the Moore Penrose pseudo-inverse of the Schur complement $\boldsymbol{\mathcal{H}}_L^{\mathrm{T}} \bar{\mathbf{R}}_{[k]}^{-1} \boldsymbol{\mathcal{H}}_L$ as follows:

$$\mathbf{M}_{L[k]}^{\star} = \breve{\mathbf{I}}_{n_\mathrm{p}} \left(\boldsymbol{\mathcal{H}}_L^{\mathrm{T}} \bar{\mathbf{R}}_{[k]}^{-1} \boldsymbol{\mathcal{H}}_L \right)^{\dagger} \boldsymbol{\mathcal{H}}_L^{\mathrm{T}} \bar{\mathbf{R}}_{[k]}^{-1} \tag{A.18}$$

In the special case where the direct transmission matrix $\mathbf{J}$ is of full rank n_p, both the Hankel matrix $\boldsymbol{\mathcal{H}}_L$ and Schur complement $\boldsymbol{\mathcal{H}}_L^{\mathrm{T}} \bar{\mathbf{R}}_{[k]}^{-1} \boldsymbol{\mathcal{H}}_L$ are of full rank $(L+1)n_\mathrm{p}$, such that the pseudo-inverse of the matrix $\boldsymbol{\mathcal{H}}_L^{\mathrm{T}} \bar{\mathbf{R}}_{[k]}^{-1} \boldsymbol{\mathcal{H}}_L$ equals its inverse. This requires at least n_p acceleration measurements (see also [16]).

Finally, note that the expression for $\mathbf{M}_{L[k]}^{\star}$ in Eq. (A.18) meets the necessary and sufficient condition for unbiased input estimation, i.e. $\mathbf{M}_{L[k]}^{\star} \boldsymbol{\mathcal{H}}_L = \breve{\mathbf{I}}_{n_\mathrm{p}}$.

Appendix A.2. State estimation

The state estimation step is given by Eq. (A.6). First, it is checked what condition the gain matrix $\mathbf{K}_{L[k]}$ should satisfy for unbiased state estimation. From Eqs. (A.1) and (A.6) it is found that the error on the state estimate $\hat{\mathbf{x}}_{[k+1|k+L]}$, denoted by $\tilde{\mathbf{x}}_{[k+1|k+L]}$, is given by:

$$\begin{aligned} \tilde{\mathbf{x}}_{[k+1|k+L]} &\triangleq \mathbf{x}_{[k+1]} - \hat{\mathbf{x}}_{[k+1|k+L]} \\ &= \mathbf{A} \tilde{\mathbf{x}}_{[k|k+L-1]} + \mathbf{B} \mathbf{p}_{[k]} + \mathbf{w}_{[k]} - \mathbf{K}_{L[k]} \tilde{\mathbf{d}}_{L[k]} \end{aligned} \tag{A.19}$$

where $\tilde{\mathbf{d}}_{L[k]} \triangleq \mathbf{d}_{L[k]} - \boldsymbol{\mathcal{O}}_{L[k]}\hat{\mathbf{x}}_{[k|k+L-1]}$. It follows from Eq. (A.3) that:

$$\tilde{\mathbf{d}}_{L[k]} = \boldsymbol{\mathcal{O}}_L\tilde{\mathbf{x}}_{[k|k+L-1]} + \boldsymbol{\mathcal{H}}_L\mathbf{p}_{L[k]} + \boldsymbol{\mathcal{N}}_L\mathbf{w}_{L-1[k]} + \mathbf{v}_{L[k]} \tag{A.20}$$

By combining Eqs. (A.19) and (A.20), the following expression for $\tilde{\mathbf{x}}_{[k+1|k+L]}$ is obtained:

$$\begin{aligned}\tilde{\mathbf{x}}_{[k+1|k+L]} = \ & (\mathbf{A} - \mathbf{K}_{L[k]}\boldsymbol{\mathcal{O}}_L)\tilde{\mathbf{x}}_{[k|k+L-1]} + (\breve{\mathbf{B}} - \mathbf{K}_{L[k]}\boldsymbol{\mathcal{H}}_L)\mathbf{p}_{L[k]}\dots \\ & + (\breve{\mathbf{I}}_{n_\mathrm{s}} - \mathbf{K}_{L[k]}\boldsymbol{\mathcal{N}}_L)\mathbf{w}_{L-1[k]} - \mathbf{K}_{L[k]}\mathbf{v}_{L[k]}\end{aligned} \tag{A.21}$$

with $\breve{\mathbf{B}} = [\mathbf{B} \quad \mathbf{0} \quad \dots \quad \mathbf{0}] \in \mathbb{R}^{n_\mathrm{s}\times(L+1)n_\mathrm{p}}$. It is immediately concluded from Eq. (A.21) that the estimator (A.6) is unbiased for all possible $\mathbf{p}_{L[k]}$ if the following equality holds:

$$\breve{\mathbf{B}} = \mathbf{K}_{L[k]}\boldsymbol{\mathcal{H}}_L \tag{A.22}$$

Assuming in addition that the initial state estimate $\hat{\mathbf{x}}_{[0|L-1]}$ is unbiased and independent of the noise processes $\mathbf{w}_{[k]}$ and $\mathbf{v}_{[k]}$ for all k, and assuming the noise processes zero mean and white, with noise covariance matrices $\mathbf{Q}$, $\mathbf{R}$, and $\mathbf{S}$ given by Eq. (A.4), the covariance matrix of the error on the state estimate $\hat{\mathbf{x}}_{[k+1|k+L]}$ is given by:

$$\mathbf{P}_{\mathrm{x}[k+1|k+L]} = \mathbf{K}_{L[k]}\bar{\mathbf{R}}_{[k]}\mathbf{K}_{L[k]}^\mathrm{T} - \mathbf{K}_{L[k]}\bar{\mathbf{S}}_{[k]}^\mathrm{T} - \bar{\mathbf{S}}_{[k]}\mathbf{K}_{L[k]}^\mathrm{T} + \bar{\mathbf{T}}_{[k]} \tag{A.23}$$

where $\bar{\mathbf{R}}_{[k]}$ is given by Eq. (A.10) and $\bar{\mathbf{S}}_{[k]}$ and $\bar{\mathbf{T}}_{[k]}$ are given by:

$$\bar{\mathbf{S}}_{[k]} = \mathbf{A}\mathbf{P}_{\mathrm{x}[k|k+L-1]}\boldsymbol{\mathcal{O}}_L^\mathrm{T} + \breve{\mathbf{I}}_{n_\mathrm{s}}\mathbf{Q}_L^0\boldsymbol{\mathcal{N}}_L^\mathrm{T} + \breve{\mathbf{I}}_{n_\mathrm{s}}\mathbf{S}_L^0 + \mathbf{A}\mathbf{P}_{\mathrm{xw}[k]}\boldsymbol{\mathcal{N}}_L^\mathrm{T} + \breve{\mathbf{I}}_{n_\mathrm{s}}\mathbf{P}_{\mathrm{wx}[k]}\boldsymbol{\mathcal{O}}_L^\mathrm{T} + \mathbf{A}\mathbf{P}_{\mathrm{xv}[k]} \tag{A.24}$$

$$\bar{\mathbf{T}}_{[k]} = \mathbf{A}\mathbf{P}_{\mathrm{x}[k|k+L-1]}\mathbf{A}^\mathrm{T} + \mathbf{Q} + \mathbf{A}\mathbf{P}_{\mathrm{xw}[k]}\breve{\mathbf{I}}_{n_\mathrm{s}}^\mathrm{T} + \breve{\mathbf{I}}_{n_\mathrm{s}}\mathbf{P}_{\mathrm{wx}[k]}\mathbf{A}^\mathrm{T} \tag{A.25}$$

The gain matrix $\mathbf{K}_{L[k]}$ that yields MVU state estimates is obtained by minimizing the trace of the error covariance matrix $\mathbf{P}_{\mathrm{x}[k+1|k+L]}$, under the constraint that Eq. (A.22) holds. Similarly to the previous section, the constraint in Eq. (A.22) is introduced in the optimization problem using Lagrange multipliers. After introduction of the constraint, the optimization problem is written as:

$$\begin{aligned}\mathbf{K}_{L[k]}^\star \ = \ & \underset{\mathbf{K}_{L[k]}\in\mathbb{R}^{n_\mathrm{s}\times(L+1)n_\mathrm{d}}}{\arg\min} \Big(\mathrm{tr}\left\{\mathbf{K}_{L[k]}\bar{\mathbf{R}}_{[k]}\mathbf{K}_{L[k]}^\mathrm{T} - \mathbf{K}_{L[k]}\bar{\mathbf{S}}_{[k]}^\mathrm{T} - \bar{\mathbf{S}}_{[k]}\mathbf{K}_{L[k]}^\mathrm{T} + \bar{\mathbf{T}}_{[k]}\right\} \\ & +2\ \mathrm{tr}\left\{(\breve{\mathbf{B}} - \mathbf{K}_{L[k]}\boldsymbol{\mathcal{H}}_L)\boldsymbol{\Lambda}_{\mathrm{x}[k]}^\mathrm{T}\right\}\Big)\end{aligned} \tag{A.26}$$

where $\boldsymbol{\Lambda}_{\mathrm{x}[k]} \in \mathbb{R}^{n_\mathrm{s}\times(L+1)n_\mathrm{p}}$ is the matrix of Lagrange multipliers. The factor 2 in the second term of the right hand side is introduced for notational convenience. Setting the derivative of the Lagrangian in Eq. (A.26) with respect to $\mathbf{K}_{L[k]}$ and $\boldsymbol{\Lambda}_{\mathrm{x}[k]}$ equal to zero yields respectively:

$$\bar{\mathbf{R}}_{[k]}\mathbf{K}_{L[k]}^\mathrm{T} - \bar{\mathbf{S}}_{[k]}^\mathrm{T} - \boldsymbol{\mathcal{H}}_L\boldsymbol{\Lambda}_{\mathrm{x}[k]}^\mathrm{T} = \mathbf{0} \tag{A.27}$$

$$\breve{\mathbf{B}} = \mathbf{K}_{L[k]}\boldsymbol{\mathcal{H}}_L \tag{A.28}$$

Eqs. (A.27) and (A.28) can be written as a linear system of equations:

$$\begin{bmatrix} \bar{\mathbf{R}}_{[k]} & -\boldsymbol{\mathcal{H}}_L \\ -\boldsymbol{\mathcal{H}}_L^{\mathrm{T}} & \mathbf{0} \end{bmatrix} \begin{bmatrix} \mathbf{K}_{L[k]}^{\mathrm{T}} \\ \boldsymbol{\Lambda}_{\mathrm{x}[k]}^{\mathrm{T}} \end{bmatrix} = \begin{bmatrix} \bar{\mathbf{S}}_{[k]}^{\mathrm{T}} \\ -\breve{\mathbf{B}}^{\mathrm{T}} \end{bmatrix} \tag{A.29}$$

The matrix $\bar{\mathbf{R}}_{[k]} \in \mathbb{R}^{(L+1)n_{\mathrm{d}} \times (L+1)n_{\mathrm{d}}}$ is nonsingular. Similar as for the input estimation step, the linear system of equations in Eq. (A.29) is solved for the gain matrix $\mathbf{K}_{L[k]}$ using the Moore Penrose pseudo-inverse of the Schur complement $\boldsymbol{\mathcal{H}}_L^{\mathrm{T}} \bar{\mathbf{R}}_{[k]}^{-1} \boldsymbol{\mathcal{H}}_L$:

$$\mathbf{K}_{L[k]}^{\star} = \bar{\mathbf{S}}_{[k]} \bar{\mathbf{R}}_{[k]}^{-1} - \left(\bar{\mathbf{S}}_{[k]} \bar{\mathbf{R}}_{[k]}^{-1} \boldsymbol{\mathcal{H}}_L - \breve{\mathbf{B}} \right) \left(\boldsymbol{\mathcal{H}}_L^{\mathrm{T}} \bar{\mathbf{R}}_{[k]}^{-1} \boldsymbol{\mathcal{H}}_L \right)^{\dagger} \boldsymbol{\mathcal{H}}_L^{\mathrm{T}} \bar{\mathbf{R}}_{[k]}^{-1} \tag{A.30}$$

Note that the expression for $\mathbf{K}_{L[k]}^{\star}$ in Eq. (A.30) meets the necessary and sufficient condition for unbiased state estimation, i.e. $\mathbf{K}_{L[k]}^{\star} \boldsymbol{\mathcal{H}}_L = \breve{\mathbf{B}}$.

Appendix A.3. Summary of the algorithm

The smoothing algorithm is initialized using an initial state estimate vector $\hat{\mathbf{x}}_{[0|L-1]}$ and its error covariance matrix $\mathbf{P}_{\mathrm{x}[0|L-1]}$. The algorithm proceeds by computing the force and state estimates recursively in two steps, i.e. the input estimation step and the state estimation step:

Input estimation

$$\mathbf{P}_{\mathrm{xw}[k]} = \sum_{i=1}^{\min(k,L)} \left(\left(\prod_{j=1}^{i-1} \left(\mathbf{A} - \mathbf{K}_{L[k-j]} \boldsymbol{\mathcal{O}}_L \right) \right) \left(\left(\breve{\mathbf{I}}_{n_{\mathrm{s}}} - \mathbf{K}_{L[k-i]} \boldsymbol{\mathcal{N}}_L \right) \mathbf{Q}_L^i - \mathbf{K}_{L[k-i]} \mathbf{S}_L^{-i^{\mathrm{T}}} \right) \right)$$

$$\mathbf{P}_{\mathrm{xv}[k]} = \sum_{i=1}^{\min(k,L)} \left(\left(\prod_{j=1}^{i-1} \left(\mathbf{A} - \mathbf{K}_{L[k-j]} \boldsymbol{\mathcal{O}}_L \right) \right) \left(\left(\breve{\mathbf{I}}_{n_{\mathrm{s}}} - \mathbf{K}_{L[k-i]} \boldsymbol{\mathcal{N}}_L \right) \mathbf{S}_L^i - \mathbf{K}_{L[k-i]} \mathbf{R}_{L+1}^i \right) \right)$$

$$\begin{aligned} \bar{\mathbf{R}}_{[k]} = {} & \boldsymbol{\mathcal{O}}_L \mathbf{P}_{\mathrm{x}[k|k+L-1]} \boldsymbol{\mathcal{O}}_L^{\mathrm{T}} + \mathbf{R}_{L+1}^0 + \boldsymbol{\mathcal{N}}_L \mathbf{Q}_L^0 \boldsymbol{\mathcal{N}}_L^{\mathrm{T}} + \boldsymbol{\mathcal{N}}_L \mathbf{S}_L^0 + \mathbf{S}_L^{0^{\mathrm{T}}} \boldsymbol{\mathcal{N}}_L^{\mathrm{T}} \dots \\ & + \boldsymbol{\mathcal{O}}_L \mathbf{P}_{\mathrm{xw}[k]} \boldsymbol{\mathcal{N}}_L^{\mathrm{T}} + \boldsymbol{\mathcal{N}}_L \mathbf{P}_{\mathrm{xw}[k]}^{\mathrm{T}} \boldsymbol{\mathcal{O}}_L^{\mathrm{T}} + \boldsymbol{\mathcal{O}}_L \mathbf{P}_{\mathrm{xv}[k]} + \mathbf{P}_{\mathrm{vx}[k]}^{\mathrm{T}} \boldsymbol{\mathcal{O}}_L^{\mathrm{T}} \end{aligned}$$

$$\mathbf{M}_{L[k]} = \breve{\mathbf{I}}_{n_{\mathrm{p}}} \left(\boldsymbol{\mathcal{H}}_L^{\mathrm{T}} \bar{\mathbf{R}}_{[k]}^{-1} \boldsymbol{\mathcal{H}}_L \right)^{\dagger} \boldsymbol{\mathcal{H}}_L^{\mathrm{T}} \bar{\mathbf{R}}_{[k]}^{-1}$$

$$\hat{\mathbf{p}}_{[k|k+L]} = \mathbf{M}_{L[k]} \left(\mathbf{d}_{L[k]} - \boldsymbol{\mathcal{O}}_L \hat{\mathbf{x}}_{[k|k+L-1]} \right)$$

$$\mathbf{P}_{\mathrm{p}[k|k+L]} = \mathbf{M}_{L[k]} \bar{\mathbf{R}}_{[k]} \mathbf{M}_{L[k]}^{\mathrm{T}}$$

State estimation

$$\bar{\mathbf{S}}_{[k]} = \mathbf{A}\mathbf{P}_{\mathrm{x}[k|k+L-1]}\boldsymbol{\mathcal{O}}_L^{\mathrm{T}} + \breve{\mathbf{I}}_{n_\mathrm{s}}\mathbf{Q}_L^0\boldsymbol{\mathcal{N}}_L^{\mathrm{T}} + \breve{\mathbf{I}}_{n_\mathrm{s}}\mathbf{S}_L^0 + \mathbf{A}\mathbf{P}_{\mathrm{xw}[k]}\boldsymbol{\mathcal{N}}_L^{\mathrm{T}} + \breve{\mathbf{I}}_{n_\mathrm{s}}\mathbf{P}_{\mathrm{xw}[k]}^{\mathrm{T}}\boldsymbol{\mathcal{O}}_L^{\mathrm{T}} + \mathbf{A}\mathbf{P}_{\mathrm{xv}[k]}$$

$$\bar{\mathbf{T}}_{[k]} = \mathbf{A}\mathbf{P}_{\mathrm{x}[k|k+L-1]}\mathbf{A}^{\mathrm{T}} + \mathbf{Q} + \mathbf{A}\mathbf{P}_{\mathrm{xw}[k]}\breve{\mathbf{I}}_{n_\mathrm{s}}^{\mathrm{T}} + \breve{\mathbf{I}}_{n_\mathrm{s}}\mathbf{P}_{\mathrm{xw}[k]}^{\mathrm{T}}\mathbf{A}^{\mathrm{T}}$$

$$\mathbf{K}_{L[k]} = \bar{\mathbf{S}}_{[k]}\bar{\mathbf{R}}_{[k]}^{-1} - \left(\bar{\mathbf{S}}_{[k]}\bar{\mathbf{R}}_{[k]}^{-1}\boldsymbol{\mathcal{H}}_L - \breve{\mathbf{B}}\right)\left(\boldsymbol{\mathcal{H}}_L^{\mathrm{T}}\bar{\mathbf{R}}_{[k]}^{-1}\boldsymbol{\mathcal{H}}_L\right)^{\dagger}\boldsymbol{\mathcal{H}}_L^{\mathrm{T}}\bar{\mathbf{R}}_{[k]}^{-1}$$

$$\hat{\mathbf{x}}_{[k+1|k+L]} = \mathbf{A}\hat{\mathbf{x}}_{[k|k+L-1]} + \mathbf{K}_{L[k]}(\mathbf{d}_{L[k]} - \boldsymbol{\mathcal{O}}_L\hat{\mathbf{x}}_{[k|k+L-1]})$$

$$\mathbf{P}_{\mathrm{x}[k+1|k+L]} = \mathbf{K}_{L[k]}\bar{\mathbf{R}}_{[k]}\mathbf{K}_{L[k]}^{\mathrm{T}} - \mathbf{K}_{L[k]}\bar{\mathbf{S}}_{[k]}^{\mathrm{T}} - \bar{\mathbf{S}}_{[k]}\mathbf{K}_{L[k]}^{\mathrm{T}} + \bar{\mathbf{T}}_{[k]}$$

References

[1] R. Adams, J. Doyle, Multiple force identification for complex structures, Experimental Mechanics 42 (2002) 25–36.

[2] L. Nordström, H. Johansson, F. Larsson, A strategy for input estimation with sensitivity analysis, International Journal for Numerical Methods in Engineering 69 (2007) 2219–2246.

[3] D. Bernal, A. Ussia, Sequential deconvolution input reconstruction, Mechanical Systems and Signal Processing 50–51 (2015) 41–55.

[4] M. Klinkov, C.-P. Fritzen, Online force reconstruction using robust observers, in: Proceedings of the Third European Workshop on Structural Health Monitoring, Granada, Spain, pp. 617–626.

[5] E. Chatzi, C. Fuggini, Structural identification of a super-tall tower by GPS and accelerometer data fusion using a multi-rate Kalman filter, in: F. Strauss, Bergmeister (Eds.), Proceedings of IALCCE 2014, 4th International Symposium on Life-Cycle Civil Engineering, Tokyo, Japan, pp. 144–151.

[6] C. Papadimitriou, C.-P. Fritzen, P. Kraemer, E. Ntotsios, Fatigue predictions in entire body of metallic structures from a limited number of vibration sensors using Kalman filtering, Structural Control and Health Monitoring 18 (2011) 554–573.

[7] A. Alessandri, M. Baglietto, G. Battistelli, Moving-horizon state estimation for nonlinear discrete-time systems: New stability results and approximation schemes, Automatica 44 (2008) 1753–1765.

[8] C.-S. Hsieh, Robust two-stage Kalman filters for systems with unknown inputs, IEEE Transactions on Automatic Control 45 (2000) 2374–2378.

[9] S. Gillijns, B. De Moor, Unbiased minimum-variance input and state estimation for linear discrete-time systems, Automatica 43 (2007) 111–116.

[10] S. Gillijns, B. De Moor, Unbiased minimum-variance input and state estimation for linear discrete-time systems with direct feedthrough, Automatica 43 (2007) 934–937.

[11] E. Lourens, E. Reynders, G. De Roeck, G. Degrande, G. Lombaert, An augmented Kalman filter for force identification in structural dynamics, Mechanical Systems and Signal Processing 27 (2012) 446–460.

[12] E. Lourens, C. Papadimitriou, S. Gillijns, E. Reynders, G. De Roeck, G. Lombaert, Joint input-response estimation for structural systems based on reduced-order models and vibration data from a limited number of sensors, Mechanical Systems and Signal Processing 29 (2012) 310–327.

[13] K. Maes, A. Smyth, G. De Roeck, G. Lombaert, Joint input-state estimation in structural dynamics, Mechanical Systems and Signal Processing 70–71 (2016) 445–466.

[14] P. Antsaklis, Stable proper nth-order inverses, IEEE Transactions on Automatic Control 23 (1978) 1104–1106.

[15] M. Sain, J. Massey, Invertibility of linear time-invariant dynamical systems, IEEE Transactions on Automatic Control 14 (1969) 141–149.

[16] K. Maes, E. Lourens, K. Van Nimmen, E. Reynders, G. De Roeck, G. Lombaert, Design of sensor networks for instantaneous inversion of modally reduced order models in structural dynamics, Mechanical Systems and Signal Processing 52–53 (2015) 628–644.

[17] T. Floquet, J.-P. Barbot, State and unknown input estimation for linear discrete-time systems, Automatica 42 (2006) 1883–1889.

[18] C.-S. Hsieh, Optimal time-delayed joint input and state estimation for systems with unknown inputs, in: Proceedings of the 48th IEEE Conference on Decision and Control, Shanghai.
[19] C.-S. Hsieh, Extension of unbiased minimum-variance input and state estimation for systems with unknown inputs, Automatica 45 (2009) 2149–2153.
[20] J. Jin, m.-J. Tahk, Time-delayed state estimator for linear systems with unknown inputs, International Journal of Control, Automation, and Systems 3 (2005) 117–121.
[21] G. Franklin, J. Powell, M. Workman, Digital control of dynamic systems, Addison-Wesley, Menlo Park, CA, 1998.
[22] J. Massey, M. Sain, Inverses of linear sequential circuits, IEEE Transactions on Automatic Control 17 (1968) 330–337.
[23] K. Maes, K. Van Nimmen, E. Lourens, A. Rezayat, P. Guillaume, G. De Roeck, G. Lombaert, Verification of joint input-state estimation for force identification by means of in situ measurements on a footbridge, Mechanical Systems and Signal Processing 75 (2016) 245–260.